The Linnean Society of London
ZOOLOGICAL Journal of the Linnean Society

Coping with the extremes: comparative osteology of the tepui-associated toad Oreophrynella and its bearing on the evolution of osteological novelties in the genus

Journal:	*Zoological Journal of the Linnean Society*
Manuscript ID	ZOJ-07-2019-3794
Manuscript Type:	Original Article
Keywords:	Lissamphibia < Taxa, osteology < Anatomy
Abstract:	The only study of the osteology of the toad genus Oreophrynella dates back to 1971 and was based on a single species. Here we use high resolution X-ray micro-computed tomography to analyse the osteology of all extant Oreophrynella species, which are compared to representatives of basal and derived bufonid lineages. Oreophrynella is unique among other bufonids in having opposable digits. Osteological synapomorphies confirmed for the genus are: presence of parietal/frontoparietal fontanelles; absence of quadratojugal; five presacral vertebrae; distally enlarged terminal phalanges; urostyle greatly expanded into flanges. Ancestral character reconstruction indicates that arboreal habits in some Oreophrynella species likely evolved following the evolution of opposable digits, arboreality possibly being an exaptation. Opposable digits, in combination with the extension of the interdigital integument, and the relative length/orientation of the digits are possible adaptations to facilitate life on tepui summits. Cranial simplification in Oreophrynella, in the form of cranial fontanelles and absence of jugal/quadratojugal, is possibly driven by a reduction of developmental costs combined with the increase in flexibility and a reduction in weight. Cranial simplification combined with the shortening of the vertebral column and the shift towards a partially firmisternal girdle might be adaptations toward the peculiar tumbling behaviour displayed by Oreophrynella

Coping with the extremes: comparative osteology of the tepui-associated toad *Oreophrynella* and its bearing on the evolution of osteological novelties in the genus

Abstract

The only study of the osteology of the toad genus *Oreophrynella* dates back to 1971 and was based on a single species. Here we use high resolution X-ray micro-computed tomography to analyse the osteology of all extant *Oreophrynella* species, which are compared to representatives of basal and derived bufonid lineages. *Oreophrynella* is unique among other bufonids in having opposable digits. Osteological synapomorphies confirmed for the genus are: presence of parietal/frontoparietal fontanelles; absence of quadratojugal; five presacral vertebrae; distally enlarged terminal phalanges; urostyle greatly expanded into flanges. Ancestral character reconstruction indicates that arboreal habits in some *Oreophrynella* species likely evolved following the evolution of opposable digits, arboreality possibly being an exaptation. Opposable digits, in combination with the extension of the interdigital integument, and the relative length/orientation of the digits are possible adaptations to facilitate life on tepui summits. Cranial simplification in *Oreophrynella*, in the form of cranial fontanelles and absence of jugal/quadratojugal, is possibly driven by a reduction of developmental costs combined with the increase in flexibility and a reduction in weight. Cranial simplification combined with the shortening of the vertebral column and the shift towards a partially firmisternal girdle might be adaptations toward the peculiar tumbling behaviour displayed by *Oreophrynella*.

ADDITIONAL KEYWORDS: Amphibia — ancestral reconstruction — heterodactyly — high resolution X-ray micro-computed tomography — tepui — Pantepui.

INTRODUCTION

The sub-cosmopolitan family Bufonidae is one of the most diverse anuran families with respect to life history traits and habitats. Bufonids inhabit a wide range of ecosystems from deserts to cloud forests, and from seashores to mountain summits as high as 5,100 m elevation (Duellman and Trueb, 1986). In addition to the well-known terrestrial toad-like phenotype, bufonids radiated repeatedly into arboreal, semi-aquatic or torrential niches/phenotypes, with reproductive modes ranging from unspecialized explosive breeding to direct development or even viviparity (Duellman and Trueb, 1986; Van Bocxlaer *et al*., 2010). One of these highly specialized genera is the genus *Oreophrynella* Boulenger, 1895 (Fig. 1), which is exclusively found on the slopes and summits of the Precambrian plateaus (named tepuis) of the western Guiana Shield. These sandstone tabletop mountains are among the most inaccessible places on earth; the highest tepuis reach nearly 3,000 m above sea level (asl) and are isolated from the surrounding lowlands by up to 1,000 m vertical cliffs (McDiarmid and Donnelly, 2005) (Fig. 2). Tepui isolation is not only physiographic, edaphic and ecological factors also contribute to further isolate most tepui summits from the surrounding savannah and tropical forest. Tepui summits are characterized by acidic, oligotrophic soils, and are exposed to high ultraviolet radiation and extreme climatic conditions, such as strong wind and high temperature variation.

The tepui region (coined “Pantepui” by Mayr and Phelps, 1967, i.e. the Guiana Shield highlands) is traditionally seen as one of the most important centres of endemism in the Neotropics (Berry *et al*., 1995; Davis *et al*., 1997). Single tepui endemism in amphibians and reptiles has been reported as exceptionally high in the region (McDiarmid and Donnelly, 2005), and it has often been suggested that tepuis are reservoirs of ancient endemism (e.g. MacCulloch and Lathrop, 2002; McDiarmid and Donnelly, 2005; Heinicke *et al*., 2009). Thorough sampling and molecular phylogenetic studies revealed that most extant tepui summit anuran species are

of relative recent origin (Kok *et al*., 2012; Salerno *et al*., 2012). Kok *et al*. (2012) showed that most tepui summit amphibian populations they studied have been subject to one or multiple instances of gene flow as recent as the Pleistocene-Holocene. This scenario contrasts with the isolation of tepui summits, but is, however, not necessarily incompatible with local ancient endemism (Kok, 2013; Kok *et al.*, 2017).

The historical biogeography of the genus was discussed by Kok *et al*. (2018), who hypothesized that the ancestor of *Oreophrynella* dispersed from the proto-Andes to the Pantepui region approximately 38 million years ago (Mya) in the late Eocene. This event roughly coincides with the divergence between the *Atelopus* + *Oreophrynella* clade and the clade consisting of *Osornophryne* + *Frostius*, the split between *Amazophrynella* + *Dendrophryniscus* from the "non-atelopodid" Bufonidae (we hereafter use the term "atelopodid" for the paraphyletic taxa branching near the base of the bufonid tree, see Kok *et al*., 2018), and a divergence event in the Pantepui frog genus *Stefania* (Kok *et al*., 2017). The timing of these events also roughly concurs with a cooling phase in the late Eocene, possibly caused by the opening of the circum-Antarctic sea (Fouquet *et al*., 2012). This combined with a major phase of mountain building in the Andean region (approximately 44 Mya; Noble *et al*., 1990), could be responsible for major ecological reorganizations across the continent and the split between most tepui-endemic herpetofauna and their sister taxa (Kok, 2013; Kok *et al*., 2018). Fouquet *et al*. (2012) suggested a correlation between the *Amazophrynella*/*Dendrophryniscus* split and climate change induced by the establishment of the Antarctic Circumpolar Current and Andean uplifts.

According to Kok *et al*. (2018), the most recent common ancestor (MRCA) of *Oreophrynella* was likely distributed throughout Pantepui, in most areas currently inhabited by extant species, before diverging into vicariant lineages. They argued that the initial diversification event probably occurred approximately 22 Mya, when the clade containing *O.*

cryptica and *O. huberi* diverged from the other *Oreophrynella* species. The most recent divergence, between *O. seegobini* and *O. weiassipuensis*, occurred as recent as approximately 0.10 Mya (Kok *et al*., 2018). Kok *et al*. (2018) recovered *Atelopus* as the sister clade of *Oreophrynella* and *Frostius* sister to *Osornophryne*. The *Atelopus* + *Oreophrynella* and *Frostius* + *Osornophryne* clades were recovered in a sister group to the remaining Bufonidae excluding *Melanophryniscus*.

The first two *Oreophrynella* species (*O. macconnelli* and *O. quelchii*) were described in the 19th century by George Albert Boulenger (1895a, 1895b, 1900). For almost a century the genus consisted of these two species only until 1990 when *O. huberi* was described by Diego-Aransay and Gorzula (1990). Since then another six species were described, of which the most recent was *O. seegobini* in 2009 (Kok, 2009). The nine currently recognized species of *Oreophrynella* occur between ca. 700-2800 m elevation, are direct developers, and have either an arboreal (three species but *O. dendronastes* has been suggested to be a junior synonym of *O. macconnelli*, see Kok, 2013) or terrestrial lifestyle (six species). To date, the genus *Oreophrynella* has been exclusively found in the eastern Pantepui region and includes species endemic to one or two tepui summits (Señaris *et al.*, 1994; McDiarmid and Donnelly, 2005; Kok *et al*., 2018). Interestingly, some tepui summit *Oreophrynella* species are phenotypically distinct but genetically very closely related (Kok *et al*., 2012; Kok *et al*., 2018). For example, pairwise distances between *O. nigra* and *O. quelchii* is 0% in 16S and only 0.63-0.95% in ND1, while *O. nigra* has a completely black ventral coloration and *O. quelchii* has a contrasting yellow-orange and black ventral colour pattern (Kok *et al*., 2012; Kok, 2013). Among bufonids, *Oreophrynella* seems to be unique in having opposable fingers and toes (Boulenger, 1895a; Señaris *et al.*, 1994; McDiarmid, 1971; Kok, 2013), a rare feature among anurans that is apparently only shared by a few genera in the family Phyllomedusidae (some members of other anuran genera, e.g. *Chiromantis*, *Pseudis*, and *Polypedates*, also possess some form of

opposability in the hands, but not nearly as extensive as in *Oreophrynella* and members of Phyllomedusidae; Sustaita *et al*., 2013). Digit opposability (hereafter referred to as "heterodactyly") has been linked to arboreality in the genus by McDiarmid (1971), who later rejected the hypothesis for tepui summit species (McDiarmid and Gorzula, 1989). To date no study has ever investigated the origin of heterodactyly in *Oreophrynella*.

Their opposable digits, small size, and thick skin easily distinguishes *Oreophrynella* from all other bufonids (Señaris *et al.*, 1994; Kok, 2013). Based on morphology alone, Kok (2009) assigned all nine species of *Oreophrynella* to four species groups, which were recovered in the molecular phylogeny of Kok *et al*. (2018).

At the time of the only available literature on the osteology of *Oreophrynella* (McDiarmid, 1971), the genera *Amazophrynella*, *Frostius*, *Metaphryniscus* and *Osornophryne* had not yet been erected. Moreover, McDiarmid (1971) based his observations on only one species (*O. quelchii*) as the number of described species of *Oreophrynella* was limited at that time. Since then an additional seven species of *Oreophrynella* have been described and recent technological advances in micro-CT scanning make it possible to gather more precise details on skeletal structures allowing a more complete and detailed overview of the osteology of *Oreophrynella*.

The present study compares the osteology of all known nine *Oreophrynella* species, as well as selected representatives of "basal" and derived bufonid lineages (11 additional species) for the purposes of (1) updating the description of the adult skeleton in *Oreophrynella* and characterising osteological synapomorphies for the genus; (2) determining the extent of osteological variation across isolated, although genetically very closely related *Oreophrynella* species; and (3) reconstructing the evolution of selected osteological characters in *Oreophrynella* and other "basal" bufonid linages (i.e. the "atelopodid" Bufonidae) under consideration of their lifestyle and environmental preferences.

MATERIAL AND METHODS

MATERIAL

We performed direct comparisons of the osteology of all known *Oreophrynella* species (nine species, 30 specimens usually of both sexes), as well as representatives of the "atelopodid" genera *Amazophrynella* (one species, one specimen), *Atelopus* (two species, two specimens), *Dendrophryniscus* (one species, one specimen), *Frostius* (one species, one specimen), *Melanophryniscus* (one species, one specimen), *Metaphryniscus* (one species, one specimen), *Osornophryne* (one species, one specimen), *Truebella* (two species, two specimens), as well as six individuals of a still undescribed bufonid species from Cerro de La Neblina at the Brazil/Venezuela border (hereafter referred as "undescribed bufonid"); see Fig. 3 for a visual summary of the "atelopodid" genera that we examined osteologically. We also directly compared the osteology of two more derived bufonid genera: *Nannophryne* (one species, one specimen) and *Rhinella* (one species, one specimen). Specimens were obtained through loans from the Museu de Zoologia, Instituto de Biologia/UNICAMP (Campinas, Brazil), the Division of Amphibians and Reptiles, National Museum of Natural History, Smithsonian Institution (Washington, USA), the Institut Royal des Sciences Naturelles de Belgique (Brussels, Belgium), and the Royal Ontario Museum (Toronto, Canada). Micro-CT scan files of the skeleton of the *Truebella* specimens were downloaded from MorphoSource (http://www.morphosource.org/) an online repository of 3D scan data, while all the other specimens were scanned for this study (Table 1). We also compared direct observations with the available literature on bufonid osteology and more particularly with the seminal work of Pramuk (2006), from which we adapted a list of 56 osteological characters used for comparison purposes (see Appendix 1).

Osteological nomenclature follows Trueb (1973, 1993) and Duellman and Trueb (1986) (see Figs 4-5). The degree of contact between structures was defined as follows: (1) free: no contact between structures; (2) contacting: contact between structures with a visible suture line; and (3) fused: contact between structures with a suture line being barely visible or absent.

HIGH RESOLUTION X-RAY MICRO-COMPUTED TOMOGRAPHY (MICRO-CT)

Micro-CT scans were acquired using the cone beam scanner HECTOR (High Energy CT Optimized for Research) (Masschaele *et al*., 2013) at the Centre for X-ray Tomography, Ghent University, Belgium (UGCT). Specimens were mounted on a stand inside a closed rectangular plastic container on top of an ethanol-saturated cloth to achieve air saturation and prevent drying of the samples during acquisition. Specimens were scanned at a tube voltage of 100 kV and target current of 0.15 mA. The PerkinElmer detector with a pixel size of 0.2 mm was used. Using geometrical magnification, a reconstructed voxel size in the range of 18-25 µm was achieved, depending on the sample size. For each scan, 2400 projection images are acquired over an angular range of 360° at an exposure time of 1 s for each image. The total scanning time per object amounted approximately 45 minutes. The raw scan data was reconstructed using the in-house developed software Octopus Reconstruction (Vlassenbroeck *et al*., 2007) (currently owned & distributed by Tescan-XRE, Ghent, Belgium) and visualized into 3D renders using the Phong volume renderer in VG STUDIO MAX 3.1 and MyVGL 3.1 software (both from Volume Graphics GmbH, Heidelberg, Germany). Images for the production of figures were taken using the built-in function in MyVGL.

ANALYTICAL METHODS

Ancestral states were inferred for "arboreality", "heterodactyly", "parietal and frontoparietal fontanelles" and "presacral vertebrae" on the well-supported time-calibrated phylogeny of "atelopodid" Bufonidae + *Nannophryne* of Kok *et al*. (2018) using R 3.5.2 for Mac OS X. Character matrices were compiled based on direct observations and descriptions from the literature (e.g. McDiarmid, 1971; Pramuk, 2006; Páez-Moscoso *et al.,* 2011; Haddad *et al.*, 2013). We reconstructed the hypothetical evolutionary history of the selected characters with stochastic character mapping (Huelsenbeck *et al.*, 2003) in *phytools* (Revell, 2012). We compared three models: an equal-rates model (ER) in which a single parameter governs all evolutionary transition rates at the same time; an all-rates-different model (ARD) where each rate is given a unique parameter; and a symmetric model (SYM) in which forward and reverse transitions share the same parameter. Model fits were compared with the likelihood ratio test (LRT) in *geiger* (Harmon *et al.*, 2008) and the best models were selected to infer the ancestral states for each trait/character. The ARD model was selected for "arboreality" and "presacral vertebrae". Both ER and SYM were suggested as best models for "heterodactyly" and "parietal and frontoparietal fontanelles" and the ER model was selected for these traits to avoid over-parameterization (results were identical anyway). Due to a lack of molecular sampling, the molecular phylogenetic position of *Metaphryniscus* and *Truebella* remains unknown.

RESULTS AND DISCUSSION

DESCRIPTION OF THE ADULT SKELETON IN *OREOPHRYNELLA*

We here describe the adult skeleton in *Oreophrynella* based on all described species in the genus (five specimens of *O. nigra*, four specimens of *O. quelchii*, five specimens of *O. vasquezi*, four specimens of *O. macconnelli*, one specimen of *O. dendronastes*, two specimens

of *O. weiassipuensis*, two specimens of *O. seegobini*, two specimens of *O. huberi*, and four specimens of *O. cryptica*). Our description updates the description provided by McDiarmid (1971).

Cranium

Sphenethmoid. The extent of ossification of the sphenethmoid varies both intra- and interspecifically. In some species, the entire nasal capsule and anterior portion of the sphenethmoid complex are reduced and unossified (e.g. *O. vasquezi*), while in other species the sphenethmoid complex is well ossified and contacting the nasals along the entire anterior margin (e.g. *O. huberi*). In some other species the ossification of the sphenethmoid extends up to halfway between the nasals (e.g. *O. seegobini*), or even up to two-thirds between the nasals (e.g. *O. weiassipuensis*). In all species the posterolateral margin of the sphenethmoid is in contact with the frontoparietal, and the sphenethmoid contacts the palatines (except in *O. dendronastes* and *O. macconnelli* as the palatines are strongly reduced) and the parasphenoid.

Prootic. The prootic is laterally overlapped by the otic ramus of the squamosal, and in medial contact with the frontoparietal. Ventrally, the prootics are in contact with the parasphenoid alae. No significant variation was noted among species.

Septomaxilla. The septomaxilla is present in all species with high intra- and interspecific variation in its shape and size. The septomaxilla appears most developed in *O. huberi* and *O. cryptica*.

Columella. The columella is absent in *Oreophrynella*.

Dorsal investing bones

Nasal. The nasals are broad, narrowly separated anteriorly, and widely separated posteriorly (except in *O. cryptica* and *O. huberi* in which the nasals are in medial contact). The acuminate posterolateral maxillary process extends ventrolaterally toward the maxilla. The maxillary

process is reduced in all *Oreophrynella* except in *O. cryptica* and *O. huberi* in which it is in contact with the maxilla. The posteromedial margin of the nasals is in contact with the sphenethmoid. The nasals are separated from the frontoparietal (except in *O. cryptica* and *O. huberi* in which the posterolateral margin of the nasals is in contact with the frontoparietal). The nasals in *O. cryptica* and *O. huberi* possess a strong dorsolateral/canthal crest that is continuous with the dorsolateral/supraorbital crest of the frontoparietal. The nasals in *O. weiassipuensis* are exostosed.

Frontoparietal. The frontoparietal possesses one roughly triangular-shaped frontoparietal fontanelle and two oval/circular parietal fontanelles. The frontoparietal contacts the sphenethmoid, is fused with the prootic, and extends laterally on each side of the frontoparietal fontanelle to the anterior level of the orbit. In *O. cryptica* and *O. huberi* the anterolateral margin of the frontoparietal is in contact with the nasals and possesses strong dorsolateral/supraorbital crests that are continuous with the dorsolateral/canthal crests of the nasals. The occipital groove is roofed over along the majority of its length (e.g. *O. weiassipuensis*) or only partially roofed (e.g. *O. cryptica*), however, this is slightly variable intra- and interspecifically.

Ventral investing and palatal bones

Parasphenoid. The parasphenoid cultriform process extends anteriorly to halfway or two-thirds of the orbit, where it is in contact with the sphenethmoid. The cultriform process narrows anteriorly to an acute tip, except in *O. cryptica* and *O. huberi* in which the cultriform process is narrow posteriorly, wide medially, and rounded anteriorly (with acute tip). A medial ridge is present in *O. cryptica* and *O. huberi*. The parasphenoid alae are generally slightly shorter than the cultriform process and are directed slightly anteriorly. The degree of contact with the pterygoid is variable intra- and interspecifically. In some species the lateral arms of the parasphenoid are in contact with the pterygoid (e.g. *O. cryptica*), while in other species there is no such contact (e.g. *O. macconnelli*).

Vomer. The extent of ossification of the vomers varies intra- and interspecifically. The postchoanal vomers are not clearly distinguishable and might be reduced/absent or incorporated into the neopalatine. The prechoanal vomers are clearly distinguishable in some species (e.g. *O. macconnelli*) and strongly reduced in some others (e.g. *O. cryptica*), widely separated, and not in contact with other structures.

Neopalatine. *Oreophrynella* possesses a relatively large palatine (except in *O. dendronastes* and *O. macconnelli* in which the palatine is strongly reduced or absent) that in ventral view extends from the anteromedial margin of the orbit, laterally and slightly posteriorly to the maxilla. There is a connection between the palatine and the maxilla on the inner surface of the latter. The palatines are widely separated, and the lateral margins are broader than the medial margins.

Maxillary arcade

Premaxilla. The medial contact of the two premaxillae is variable intra- and interspecifically. In some species the premaxillae are separated medially (e.g. *O. macconnelli*) while in other species there is medial contact (e.g. *O. weiassipuensis*). The alary processes diverge from the midline and are directed dorsally (e.g. *O. vasquezi*) or anterodorsally (e.g. *O. seegobini*). The degree of lateral contact between the premaxillae and the maxillae is variable intra- and interspecifically. In some species there is no contact between the premaxillae and the maxillae (e.g. *O. macconnelli*) and in some species there is minimal contact (e.g. *O. weiassipuensis*).

Maxilla. The maxilla is long with both the pars fascialis and the pars palatina being poorly developed. The posterior margin of the maxilla is acute along the ventral margin and rises rapidly at about a 45-70° angle to the pterygoid portion and thence nearly straight across up to the anterior margin. The maxilla in *O. cryptica*, *O. huberi*, *O. seegobini*, and *O. weiassipuensis* possesses a posterodorsal projection directed towards the orbital/zygomatic ramus of the squamosal, which is greatly expanded in these species. The posterodorsal projection of the

maxilla in *O. cryptica* and *O. huberi* is in contact with the orbital/zygomatic ramus of the squamosal. The exostosis on the dorsolateral margin of the maxilla in *O. seegobini* and *O. weiassipuensis* forms a distinct suborbital crest.

Suspensory apparatus

Pterygoid. The triradiate pterygoid bears a curved anterior ramus that is in contact with the dorsomedial margin of the maxilla. The posterior ramus is broad, flat, and rounded. The degree of contact of the medial ramus with the prootic and the parasphenoid is variable intra- and interspecifically. The posterior and medial rami are approximately of equal length.

Quadratojugal. The quadratojugal is absent in *Oreophrynella*.

Squamosal. The ventral ramus of the squamosal extends from the angulosplenial to the posterodorsal margin of the orbit. The narrow ventral ramus is straight or slightly curved and laterally flattened. Great intra- and interspecific variation exists in the shape of the otic and zygomatic rami. The otic ramus extends over the lateral margin of the prootic and onto its dorsal surface. The otic ramus is longer than the zygomatic ramus (except in *O. cryptica*, *O. huberi*, *O. seegobini* and *O. weiassipuensis*). The zygomatic ramus in *O. cryptica* and *O. huberi* forms an orbital branch that extends anteroventrally to contact the maxilla posterodorsally. The otic ramus in these species is extended posterodorsally. A flange is present between the otic and zygomatic rami. A pretympanic/postorbital crest is present on the zygomatic ramus of the squamosal in *O. cryptica* and *O. huberi*. A supratympanic crest is present on the otic ramus of the squamosal in *O. seegobini*, *O. weiassipuensis*, *O. cryptica*, and *O. huberi*. The squamosal in *O. seegobini* and *O. weiassipuensis* is fairly similar to the squamosal in *O. cryptica* and *O. huberi*. However, in *O. seegobini* and *O. weiassipuensis* the orbital branch is not in contact or only in minimal contact with the maxilla. The otic and zygomatic rami in these species are exostosed (most prominently in *O. weiassipuensis*). The otic ramus in *O. dendronastes* is directed posterodorsally.

Mandible

Mentomeckelian. Mentomeckelians are small and arcuate in ventral view, medially broadened, separated medially, and laterally contacting the dentaries.

Dentary. The dentary is long and slim, posteriorly acuminate, and broadening anteriorly, where it contacts the mentomeckelian. The dentary overlaps the angulosplenial for most of its length.

Angulosplenial. The angulosplenial is long and arcuate, acuminate anteriorly, and broad and rounded posteriorly. The posterior ramus is shorter in *O. cryptica* and *O. huberi*, and longer in *O. dendronastes*. The coronoid process is best developed in *O. dendronastes*, *O. macconnelli*, *O. seegobini*, and *O. weiassipuensis*.

Postcranium

Vertebral column. There are five presacral vertebrae present, each with round posterior articulate processes/postzygapophyses (more rectangular in *O. dendronastes*). The cervical vertebra (presacral I) is fused with the first trunk vertebra (presacral II). This fusion results in a cervical vertebra with transverse processes (atlas complex). A 'ʎ'-shaped ridge is present on the neural arch of the vertebrae. The length of the transverse processes in most species is II>III>I=V=IV, but in *O. cryptica* and *O. huberi* is III>II>IV=V>I. The transverse processes of presacral II are broadest. Transverse processes of presacral I are directed anteroventrally; transverse processes of presacral II and III are directed posteroventrally; transverse processes of presacral IV are directed ventrally and roughly perpendicular to the medial axis; and transverse processes of presacral V are directed slightly anteroventrally. The vertebrae in *O. dendronastes* are slenderer than those in other *Oreophrynella*, while the 'ʎ'-shaped ridge appears more pronounced and slenderer at the same time.

Sacrum. The sacrum likely includes two trunk vertebrae, clearly shown by the presence of spinal nerve foramina on the ventral part of the sacrum. However, the number of spinal nerve foramina is variable intra- and interspecifically, likely due to variation in the extent of

ossification. The sacrum bears flattened and greatly expanded diapophyses, which distally contact the ilia. The anterior margins of the sacral diapophyses are directed anterolaterally and their lateral margins are rounded and shaped like an axe head. Posteriorly, the sacrum is broadly fused with the urostyle. A medial sacral ridge, which extends onto the urostyle, is present.

Urostyle. The urostyle is approximately the same length as the vertebral column (presacral I-V). The urostyle is fused to the sacrum and bears a greatly expanded lateral flange that extends from the posterolateral margin of the sacral diapophyses posteromedially almost to the posterior tip of the urostyle. However, in some species this expansion is greater than in other species. The expansion is least in *O. dendronastes* and *O. macconnelli*, slightly more expanded in *O. nigra*, *O. quelchii*, and *O. vasquezi*, more expanded again in *O. cryptica* and *O. huberi*, and best developed in *O. seegobini* and *O. weiassipuensis*. A low, but well-defined, dorsal ridge is present in all species.

Pectoral girdle. The clavicles are directed anteriorly and are nearly straight to slightly curved, with their truncate medial tips narrowly separated. The coracoids are separated and expanded medially, with the sternal end much broader than the glenoid end. The posterior border is nearly straight, while the anterior border is strongly curved. The pars acromialis of the scapula is clearly distinct from the pars glenoidalis, but they are approximately equal in length. The suprascapulae are well ossified, with their anterior borders straight and their posterior borders curved. They are widely separated medially.

Forelimb and manus. The humerus bears a ventral and a lateral ridge. The ventral ridge is present on the proximal 25% of the humerus and continues on the caput humeri. The lateral ridge is less prominent. The radioulna is quite broad. The sulcus intermedius is indicated by a distinct groove. The carpus is composed of a radiale, ulnare, ossified prepollex element, element Y, carpal 2, and an element representing the fusion of carpals 3-5. A sesamoid bone is present on the ventral side of the element representing carpals 3-5 (Fig. 6). Metacarpals

increase in size, generally in the following order: 1, 4, 2, 3. The finger phalangeal formula is standard (2-2-3-3). The distal phalanges are expanded into a 'T'-shape (most pronounced in *O. dendronastes* and *O. macconnelli*). The fingers are widely separated and relatively similar in length. Length of fingers: III>II=IV>I.

Pelvic girdle. The iliac shafts are almost cylindrical with a prominent dorsal crest. The ilia pass ventrolateral to the sacrum, where there is contact between these two structures. The ilia are posteriorly fused to the ischium and form a 'U'-shape in ventral view. The pubis is ossified.

Hindlimb and pes. The femur and tibiofibula are approximately of equal length. The femur is nearly straight and bears a ventral ridge on its proximal end. The sulcus intermedius of the tibiofibula is less prominent than the sulcus intermedius of the radioulna. The astragalus and calcaneum are slightly shorter than the femur and tibiofibula. These structures are widely separated at their midpoint and fused at their distal and proximal heads. Three tarsals – T1 T2, and T3 – are present at base of digits I, II, and III. An element Y and an elongate ossified prehallux element are also present (Fig. 7). Metatarsals 1, 2 and 3 are of similar length, slightly shorter than metatarsals 3 and 4, which are subequal. The toe phalangeal formula is standard (2-2-3-4-3). The distal phalanges are expanded into a 'T'-shape (most pronounced in *O. dendronastes* and *O. macconnelli*). The toes are widely separated and relatively similar in length. Length of toes: IV>V>I=II=III.

OSTEOLOGICAL SYNAPOMORPHIES IN *OREOPHRYNELLA*

We identified the following unambiguous osteological synapomorphies in *Oreophrynella*: presence of parietal fontanelles; presence of frontoparietal fontanelles; absence of quadratojugal; five presacral vertebrae; distally enlarged terminal phalanges; urostyle greatly expanded into flanges.

Of the 56 osteological characters that we employed for comparison (mostly based on Pramuk, 2006, see Appendix 1), two are unique to the genus *Oreophrynella*: characters 10 and 11 (i.e. the presence of parietal and frontoparietal fontanelles). Even more striking are the feet in *Oreophrynella*, which differ considerably from those in anurans, let alone other bufonid genera. The toes in *Oreophrynella* are widely separated to form a fan-like shape, whereas the toes in other bufonid genera are oriented roughly perpendicular to the calcaneum/astragalus. The angle between the first and last toe in *Oreophrynella* is ca. 160°, which angle varies from ca. 30-80° in other bufonid genera we examined (see Fig. 7). The digits are similar in length and widely separated. In *Oreophrynella* Toe I is subequal to Toes II and III, whereas Toe I is the shortest toe in all other bufonid genera we examined. Figure 7 also shows the distally expanded terminal phalanges in *Oreophrynella*, which is greatest in *O. macconnelli* and *O. dendronastes*.

Character 34 (five presacral vertebrae) is shared with just one of the species examined, the undescribed bufonid. Likewise, *Oreophrynella* only shares character 40 (greatly expanded flanges on urostyle) with at least three of the genera examined: *Osornophryne bufoniformis*, *Metaphryniscus sosai*, and the undescribed bufonid. Table 2 displays the taxa by character matrix used for the osteological comparison (see Appendix 1 for character descriptions). The other 54 character states are shared with at least one representative of the genera examined in this analysis.

McDiarmid (1971) identified three unique osteological characters in the genus (based solely on *Oreophrynella quelchii*, see above): (1) the presence of parietal and frontoparietal fontanelles (confirmed here based on a larger dataset); (2) the fusion of the sacrum and trunk vertebrae; and (3) the incomplete ossification of the sphenethmoid complex (ossification restricted to the poster section). The last two characters are not recovered as unique for the genus in our analyses. Indeed, the fusion of the sacrum with trunk vertebrae – indicated by the

presence of spinal nerve foramina (see Noble, 1926; McDiarmid 1971) – also occurs in specimens of at least *Osornophryne*, *Frostius*, *Dendrophryniscus*, and *Metaphryniscus*. The ossification of the sphenethmoid complex appears to vary intra- and interspecifically, and some of the *Oreophrynella* specimens (e.g. *O. cryptica* and *O. huberi*) we examined showed extensive ossification of the sphenethmoid complex.

OSTEOLOGICAL VARIATION AMONG *OREOPHRYNELLA* SPECIES

Kok (2009) assigned all nine species of *Oreophrynella* to four unnamed species groups, mostly based on external morphology. These groups were later recovered in the molecular phylogeny of Kok *et al*. (2018) and we take the opportunity to formally name them hereafter. Although discrete species identification based on osteological characters is difficult (if ever possible; see below), the four *Oreophrynella* species groups proposed by Kok (2009) are easily differentiated by their distinctive cranial osteology (Figs 8-10).

Oreophrynella cryptica and *O. huberi* (the *O. huberi* species group) are most easily distinguished from the three other *Oreophrynella* groups by the medial contact of the nasals (no contact in other species), dorsolateral contact between the nasals and the frontoparietal (no contact in other species), expansion of the maxillary process of the nasal (less expanded in other species), broad shape and medial ridge of cultriform process of the parasphenoid (narrow and ridge absent in other species), expansion of the otic ramus of the squamosal (not or poorly expanded in other species), and presence of canthal, parietal, pretympanic/postorbital, and supraorbital crests (absent or less marked in other species). These two species can also be distinguished by the contact between the zygomatic ramus of the squamosal and the maxilla, however very minimal contact between these two structures is also observed in one specimen of *O. weiassipuensis*. Furthermore, *O. cryptica* and *O. huberi* differ from *O. nigra*, *O. quelchii*,

and *O. vasquezi* by the anterodorsal orientation of the alary process of the premaxilla (dorsally directed in *O. nigra*, *O. quelchii*, and *O. vasquezi*); from *O. seegobini* and *O. weiassipuensis* by a non-exostosed suborbital crest (exostosed in *O. seegobini* and *O. weiassipuensis*) and the absence of exostosis on the dermal roofing bones (present in *O. seegobini* and *O. weiassipuensis*); and from *O. macconnelli* and *O. dendronastes* by the presence of a supratympanic crest on the otic ramus of the squamosal (absent in *O. macconnelli* and *O. dendronastes*) and the presence of the palatine (absent/reduced in *O. macconnelli* and *O. dendronastes*).

Oreophrynella seegobini and *O. weiassipuensis* (the *O. weiassipuensis* species group) can be distinguished from the three other *Oreophrynella* groups by the presence of exostosis on the dermal roofing bones (absent in other species) and the presence of an exostosed suborbital crest (absent or less developed and non-exostosed in other species). In addition, *O. seegobini* and *O. weiassipuensis* differ from *O. nigra*, *O. quelchii*, and *O. vasquezi* by the great expansion of the zygomatic ramus of the squamosal (not or minimally expanded in *O. nigra*, *O. quelchii*, and *O. vasquezi*), the anterodorsal orientation of the alary process of the premaxilla (dorsally directed in *O. nigra*, *O. quelchii*, and *O. vasquezi*), and the presence of exostosis on the otic ramus of the squamosal (absent in *O. nigra*, *O. quelchii*, and *O. vasquezi*); from *O. macconnelli* and *O. dendronastes* by the great expansion of the zygomatic ramus of the squamosal (not or minimally expanded in *O. macconnelli* and *O. dendronastes*), the presence of the palatine (absent/reduced in *O. macconnelli* and *O. dendronastes*), and the presence of exostosis on the otic ramus of the squamosal (absent in *O. macconnelli* and *O. dendronastes*); and from *O. cryptica* and *O. huberi* by the lack of contact between nasals (contact in *O. cryptica* and *O. huberi*), lack of contact between nasals and frontoparietal (contact in *O. cryptica* and *O. huberi*), narrow shape and lack of a medial ridge on the cultriform process of the parasphenoid

(shape broad and medial ridge present in *O. cryptica* and *O. huberi*), and the absence of canthal, parietal, pretympanic/postorbital, and supraorbital crests (present in *O. cryptica* and *O. huberi*).

Oreophrynella nigra, *O. quelchii*, and *O. vasquezi* (the *O. quelchii* species group) can be distinguished from the three other *Oreophrynella* groups by the dorsal orientation of the alary process of the premaxilla (directed anterodorsally in the other species). Furthermore, *O. nigra*, *O. quelchii*, and *O. vasquezi* differ from *O. seegobini*, *O. weiassipuensis*, *O. cryptica* and *O. huberi* by the lack of expansion of the zygomatic ramus of the squamosal (expanded in *O. seegobini*, *O. weiassipuensis*, *O. cryptica* and *O. huberi*) and from *O. seegobini* and *O. weiassipuensis* by the absence of exostosis on the otic ramus of the squamosal (present in *O. seegobini* and *O. weiassipuensis*); and from *O. macconnelli* and *O. dendronastes* by the presence of the palatine (reduced in *O. macconnelli* and *O. dendronastes*).

Oreophrynella macconnelli and *O. dendronastes* (the *O. macconnelli* species group) can be distinguished from the three other *Oreophrynella* groups by the reduction of the palatine (not reduced in the other species) and the shape of the terminal phalanges ("T-shape" less broad in other species), which could be an adaptation towards their arboreal lifestyle. In addition, *O. macconnelli* and *O. dendronastes* differ from *O. seegobini*, *O. weiassipuensis*, *O. cryptica* and *O. huberi* by the minimal, or lack of, expansion of the zygomatic ramus of the squamosal (greatly expanded in *O. seegobini*, *O. weiassipuensis*, *O. cryptica* and *O. huberi*) and from *O. seegobini* and *O. weiassipuensis* by the absence of exostosis on the otic ramus of the squamosal (present in *O. seegobini* and *O. weiassipuensis*); and from *O. cryptica* and *O. huberi* by the absence of a supratympanic crest on the otic ramus of the squamosal (present in *O. cryptica* and *O. huberi*).

Kok *et al*. (2012) highlighted phenotypical differences between some closely related *Oreophrynella* species despite their extremely low genetic divergence. Our results indicate that osteological differences are very minimal or absent between genetically very close species (i.e.

O. quelchii/*O. nigra*, *O. weiassipuensis*/*O. seegobini*, *O. huberi*/*O. cryptica*, and *O. macconnelli*/*O. dendronastes*). Compared with *Oreophrynella nigra*, the posterior part of the occipital groove is usually covered ("closed") in *O. quelchii* (usually not covered in *O. nigra*) and the surface of the otic and zygomatic ramus of squamosal is relatively smooth in *O. quelchii* (more irregular in *O. nigra*); compared with *O. seegobini*, *O. weiassipuensis* has the skull more heavily ornamented/exostosed, the nasals more widely separated, the parietal fontanelles smaller and more irregular in shape (circular in *O. seegobini*), the orbital branch of the squamosal nearly in contact with the maxilla (greater distance between squamosal and maxilla in *O. seegobini*), some mineralization between the angulosplenial and the dentary (absent in *O. seegobini*), and the lateral edges of the sacral diapophysis slightly rounded (nearly straight in *O. seegobini*). The diagnostic value of these osteological characters should be tested on a larger sample size to rule out intraspecific variation. No unambiguous diagnostic osteological feature could be identified between *O. huberi* and *O. cryptica*, and between *O. macconnelli* and *O. dendronastes*.

ANCESTRAL STATE RECONSTRUCTION AND OSTEOLOGICAL NOVELTIES IN *OREOPHRYNELLA*

According to Kok *et al*. (2018), the ancestor of *Oreophrynella* dispersed from the proto-Andes to the Pantepui region approximately 38 Mya. Our results confirm the anticipated assumption that characters unique to *Oreophrynella* such as digit opposability and the presence of frontoparietal and parietal fontanelles, as well as the reduction to five presacral vertebrae are likely to have evolved after that jump-dispersal event (Fig. 11).

It remains unclear what factors contributed to — and selected for — the unique adaptations present in *Oreophrynella*. McDiarmid (1971) once hypothesized that digit opposability in

Oreophrynella might reflect a partially arboreal lifestyle. However, this seems questionable as, although anecdotic records of the use of low arboreal shelter in terrestrial *Oreophrynella* species exist (e.g. Mourthe *et al.*, 2017; the authors, pers. obs.), only three *Oreophrynella* species (or two, as *O. dendronastes* has been suggested to be a junior synonym of *O. macconnelli*; Kok 2013) have true arboreal habits (i.e. these species spend most of their time in trees and/or bushes; the authors, pers. obs.). Besides, there is a plethora of arboreal anurans that lack opposable toes (e.g. other arboreal members of the family Bufonidae, members of the families Centrolenidae, Hylidae, Hyperoliidae, Mantellidae, and Rhacophoridae), so the selective advantage of opposable toes for arboreality in anurans is not obvious. Strikingly, the three *Oreophrynella* species with arboreal habits occupy a similar upland/highland habitat consisting in (sub-)montane wet tropical forest, while the six terrestrial *Oreophrynella* species occur in high montane tepui summit habitats (Kok, 2009; Kok *et al.*, 2018; Lathrop and MacCulloch, 2007; Señaris *et al.*, 2005). Kok (2013) hypothesized that the ancestor of *Oreophrynella* could have been terrestrial, arboreality possibly being an exaptation. Our results concur with that hypothesis, showing that instead of opposability being an adaptation towards an arboreal lifestyle, arboreal habits in *Oreophrynella* likely evolved following the evolution of opposable digits, with no correlation found between heterodactyly and arboreality in "atelopodid" Bufonidae (>99% relative probability for the MRCA of *Atelopus* + *Oreophrynella* having non-opposable digits; 84.7% relative probability for the ancestor of *Oreophrynella* being terrestrial, Fig. 10A, B). Kok (2013) also suggested that opposability could be an adaptation to rock climbing, which seems likely as part of *Oreophrynella* habitat consists of bare rock, crevices, and outcrops. This combined with the extension of the interdigital integument (which differs significantly from webbing in other anurans; Señaris *et al.*, 2005), the relative length of the digits (more similar in length compared to other anurans), the orientation of the digits (digits widely separated), and the reduction in the number of vertebrae

could all be adaptations to facilitate life on tepui summits. Indeed, the extension of the interdigital integument and the orientation of the digits increase surface area, and likely also increase contact area with the substrate and grip. Likewise, a walking locomotion coupled with heterodactyly is probably an advantage when moving on rocks and in the thick ground vegetation of tepui summits.

Even if the correlation is not obligatory, intercalary elements (additional structures between the ultimate and penultimate phalanx), adaptations in tendon and muscle complexes, adhesive digital pads, and distally enlarged terminal phalanges are often present in species with climbing habits (not necessarily arboreal, Manzano *et al*., 2008; Kamermans and Vences, 2009). All *Oreophrynella* species have adhesive digital pads (the authors, pers. obs.), and although the terminal phalanges are expanded to form a "T-like" shape in all *Oreophrynella* species, they are significantly more expanded in *O. macconnelli* and *O. dendronastes*, which could indicate an adaptation to their arboreal lifestyle. Likewise, there is a substantial reduction of interdigital integument in these two species. In the third arboreal *Oreophrynella* species, *O. weiassipuensis*, however, the shape of the terminal phalanx and the extent of interdigital integument are similar to that of its terrestrial congeners. This might be explained by the relatively recent split between *O. weiassipuensis* and *O. seegobini* (approximately 0.10 Mya according to Kok *et al*., 2018), while *O. macconnelli* and *O. dendronastes* diverged relatively long ago (approximately 16.12 Mya according to Kok *et al*., 2018) and thus had more time to evolve. Also, *O. weiassipuensis* lives in low bushes (the authors, pers. obs.), while *O. macconnelli* and *O. dendronastes* are found higher in trees (Lathrop and MacCulloch, 2007; Kok, 2009). Unfortunately, Micro-CT scans do not render soft tissue well (e.g. cartilages, muscles and tendons) and therefore we could not draw inferences on adaptations present in these tissue types. Further research on intercalary elements and muscular complexes is

necessary to determine which adaptations facilitate opposability in *Oreophrynella*, as well as its benefits and constraints.

The frontoparietal in adult *Oreophrynella* appears as two segments that are fused only posteriorly due to the incomplete metamorphosis of this bone, which leaves the frontal and frontoparietal fontanelles exposed. The presence of these fontanelles is a paedomorphic character unique to *Oreophrynella*. Juveniles of many other species of bufonid display frontoparietal and parietal fontanelles (e.g. Jorgensen and Sheil, 2008; Rodrigues de Oliveira *et al*., 2014), which are closed during later stages of development. Griffiths (1954) investigated the developmental patterns of metamorphosis of the frontoparietal in *Rhinella marina*, and McDiarmid (1971) noted that the same basic metamorphic patterns of frontoparietal development present in *Rhinella marina* also occur in *Atelopus* (sister genus to *Oreophrynella*). Therefore, McDiarmid assumed that the MRCA of *Atelopus* + *Oreophrynella* exhibited a similar pattern of metamorphosis and that the adult had a well-developed frontoparietal bone. This assumption is confirmed by our ancestral state reconstruction (>99% relative probability for the MRCA of *Atelopus* + *Oreophrynella* lacking fontanelles, Fig. 10C). In *Oreophrynella*, the ancestral adult condition has been substituted by a paedomorphic trait through modification of the ontogeny. The evolutionary or functional significance of this differential metamorphosis is still unknown (McDiarmid, 1971) and worthy of discussion. Interestingly, an explanation for the function of the fontanelles in *Oreophrynella* might be found in salamanders. Zhou *et al*. (2017) discussed the evolutionary and developmental implications of the cranial biomechanics in basal urodeles. These authors state that the appearance of cranial fontanelles may be related with cranial simplification. This simplification could be a consequence of biomechanical optimization, which might imply a reduction of developmental costs, with potential benefits for an ectothermic species living in extreme conditions (which also is the case for most extant *Oreophrynella*). This bone loss trend is also evident in the absence of the jugal/quadratojugal

bone, which, when present, stabilizes the skull. This stabilizing role in taxa without a jugal/quadratojugal is fulfilled by a jugal ligament, which has the same function of stabilizing the skull. These changes in ontogeny imply a major increase in flexibility, possibly helping to distribute stress through the skull (Zhou *et al*., 2017). The presence of fontanelles and the absence of the quadratojugal in *Oreophrynella* might indicate the presence of similar basic ossification patterns as in basal salamanders. The advantages of the reduction of developmental costs combined with the increase in flexibility coupled to a reduction in weight may be driving forces behind the simplification of the cranial osteology in *Oreophrynella*. This increased flexibility hypothesis needs to be tested in future research, for example through stress test of the *Oreophrynella* skull.

McDiarmid (1971) suggested that the reduction in the number of vertebrae could be linked to walking locomotion. However, an increase in rigidity of the vertebral column seems to favour saltatory instead of walking locomotion. Such a correlation between a low number of presacral vertebrae and walking locomotion is not striking in "atelopodid" Bufonidae since most of them are walkers/hoppers instead of jumpers. Our ancestral state reconstruction indicates that the reduction of presacral vertebrae evolved at least five times independently in "atelopodid" bufonids and that the MRCA of *Atelopus* + *Oreophrynella* most likely had 8 presacral vertebrae (100% relative probability, Fig. 10D), reduced to seven in *Atelopus* and to five in *Oreophrynella*. The only "atelopodid" species in which we also found a reduction to five presacral vertebrae is the undescribed bufonid from Cerro La Neblina at the border between Brazil and Venezuela, which is also a species restricted to Pantepui. It is worth mentioning that in "atelopodid" bufonids a correlation is observed between a strong reduction of presacral vertebrae (≤ 6) and direct development (Fig. 10D). Another feature that is probably correlated with the shortening of the vertebral column is the shift towards a (partially) firmisternal girdle. In this type of pectoral girdle, a more rigid combination of the two halves

of the pectoral girdle provides additional support for the limbs. These derived character states in the genus *Oreophrynella* would contribute to increase rigidity along the longitudinal axis of the body.

The added rigidity from the shortening of the vertebral column and the shift towards a partially firmisternal girdle combined with the added flexibility from the cranial simplification might be adaptations toward the peculiar "tumbling behaviour" displayed by *Oreophrynella*. This behaviour is used in escaping predators (Holmes and Gunton, 2009; the authors, pers. obs.). *Oreophrynella nigra* individuals are best known to recklessly throw themselves downhill when disturbed. While tumbling down steep rock faces, the toads come into contact with the rock multiple times, which must exercise great forces onto the head and body. Thus, the adaptations mentioned earlier could also have evolved to protect the head and body from fatal injuries during this tumbling behaviour. Remarkably, this tumbling behaviour is also present in other terrestrial *Oreophrynella* species (likely all, the authors, pers. obs.), and a comparable behaviour has even been observed in arboreal species of the genus. Indeed, stressed individuals of *O. macconnelli* for instance, jump from tree branches or leaves, free-falling amid other branches until they are able to grab one (Holmes and Gunton, 2009). Here again toads may strongly hit several obstacles, such as large leaves and branches, before being able to stop their fall.

Some additional insights about cranial shock absorption might be found in mammals. Fontanelles and sutures in human infants for instance allow the head to deform during childbirth. These fontanelles and sutures also absorb significantly more energy during impact than cranial bone, confirming the shock-absorbing role of the fontanelles and sutures in the paediatric skull (Jaslow, 1990). Paediatric cranial suture can deform up to 243 times more than adult cranial bone. This significant difference underscores the essential role that fontanelles and sutures play in the response of the paediatric head to impact (Coats and Margulies, 2006;

Margulies and Thibault, 2000; Wood, 1971). Fontanelles in human infants are located between the several bones that make up the skull. These fontanelles are covered with suture material, which connects the several bones and gives elasticity to the entire skull (Coats and Margulies, 2006). In *Oreophrynella*, however, only the frontoparietal fontanelle is located between bones, namely the frontoparietal and the sphenethmoid, while the parietal fontanelles are not located between different structures but within one bone, namely the frontoparietal. So even though fontanelles and sutures appear to play a different role in human infants, they might give a clue about the role and function of fontanelles in *Oreophrynella*.

CONCLUSION

Our study provides details of the osteological structures in the bufonid genus *Oreophrynella*. We have highlighted evidence correlating the evolution of osteological novelties in *Oreophrynella* with the adaptation to the unique environment of Pantepui, even if the function of some of these novelties remains speculative. This is in line with the hypothesis of some Pantepui lineages locally evolving on a large tepui-like plateau that was later gradually dissected into isolated tepuis (e.g. Kok *et al*., 2017).

REFERENCES

Berry PE, Huber O, Holst BK. 1995. Floristic analysis and phytogeography. In: Berry PE, Holst BK, Yatskievych K, eds. *Flora of the Venezuelan Guayana. Volume 1. Introduction*. St Louis: Missouri Botanical Garden Press, pp. 161–192.

Boulenger GA. 1895a. Description of a new Batrachian (*Oreophryne quelchii*) discovered by Messrs. J.J. Quelch & F. McConnell on the summit of Mount Roraima. *Annals and Magazine of Natural History, Series 6* **15:** 521–522.

Boulenger GA. 1895b. Correction to p. 521 ("Annals", June 1895). *Annals and Magazine of Natural History*, *Series 6* **16:** 125.

Boulenger GA. 1900. Batrachians. Report on a collection made by Messrs. F.V. McConnell and J.J. Quelch at Mount Roraima in British Guiana. *Transactions of the Linnean Society of London*, Zoology, *Series 2* **8:** 55–56.

Coats B, Margulies SS. 2006. Material properties of human infant skull and suture at high rates. *Journal of Neurotrauma* **23(8):** 1222–1232.

Davis SD, Heywood VH, Hamilton AC. 1997. *Centres of Plant Diversity: A Guide and Strategy for their Conservation, Volume 3, The Americas*. IUCN Publications Unit, Cambridge, 1–562.

Diego-Aransay A, Gorzula S. 1990 "1987". Una nueva especie de *Oreophrynella* (Anura: Bufonidae) de la Guayana Venezolana. *Memoria de la Sociedad de Ciencias Naturales La Salle* **127/128:** 233–238.

Duellman WE, Trueb L. 1986. *Biology of amphibians*. McGraw-Hill Book Company, New York, 1–670.

Fouquet A, Recoder R, Teixeira M, Cassimiro J, Amaro RC, Camacho A, Damasceno R, Carnaval AC, Moritz C, Rodrigues MT. 2012. Molecular phylogeny and morphometric analyses reveal deep divergence between Amazonia and Atlantic forest species of *Dendrophryniscus*. *Molecular Phylogenetics and Evolution* **62:** 826–838.

Griffiths I. 1954. On the nature of the frontoparietal in Amphibia, Salientia. *Proceedings of the Zoological Society of London* **123:** 781–792.

Haddad CFB, Toledo LF, Prado CPA, Loebmann D, Gasparini JL, Sazima I. 2013. *Guia dos anfíbios da Mata Atlântica: diversidade e biologia*. Anolis Books, São Paulo.

Harmon LJ, Weir J, Brock C, Glor RE, Challenger W. 2008. GEIGER: investigating evolutionary radiations. *Bioinformatics* **24:** 961–964.

Heinicke MP, Duellman WE, Trueb L, Means DB, MacCulloch RD, Hedges SB. 2009. A new frog family (Anura: Terrarana) from South America and an expanded direct-developing clade revealed by molecular phylogeny. *Zootaxa* **2211:** 1–35.

Holmes, M. and M. Gunton. 2009. *Life, Extraordinary Animals, Extreme Behavior*. United Kingdom: BBC Natural History Unit & The Open University.

Huelsenbeck JP, Nielsen R, Bollback JP. 2003. Stochastic mapping of morphological characters. *Systematic Biology* **52:** 131–158.

Jaslow CR. 1990. Mechanical Properties of Cranial Sutures. *Journal of Biomechanics* **23(4):** 313–321.

Jorgensen ME, Sheil CA. 2008. Effects of temperature regime through premetamorphic ontogeny on shape of the chondrocranium in the American toad, *Anaxyrus americanus*. *The Anatomical Record* **291:** 818–826.

Kamermans M, Vences M. 2009. Terminal phalanges in ranoid frogs: morphological diversity and evolutionary correlation with climbing habits. *Alytes* **26:** 117–152.

Kok PJR. 2009. A new species of *Oreophrynella* (Anura: Bufonidae) from the Pantepui region of Guyana, with notes on *O. macconnelli* Boulenger, 1900. *Zootaxa* **2071:** 35–49.

Kok PJR. 2013. Islands in the Sky: Species Diversity, Evolutionary History, and Patterns of Endemism of the Pantepui Herpetofauna. PhD thesis, Leiden University, The Netherlands.

Kok PJR, MacCulloch RD, Means DB, Roelants K, Van Bocxlaer I, Bossuyt F. 2012. Low genetic diversity in tepui summit vertebrates. *Current Biology* **22(15):** 589–590.

Kok PJR, Ratz S, MacCulloch RD, Lathrop A, Dezfoulian R, Aubret F, Means DB. 2018. Historical biogeography of the palaeoendemic toad genus *Oreophrynella* (Amphibia: Bufonidae) sheds a new light on the origin of the Pantepui endemic terrestrial biota. *Journal of Biogeography* **44:** 26–36.

Kok PJR, Russo VG, Ratz S, Means DB, MacCulloch RD, Lathrop A, Aubret F, Bossuyt F. 2017. Evolution in the South American 'Lost World': Insights from multilocus phylogeography of stefanias (Anura, Hemiphractidae, *Stefania*). *Journal of Biogeography* **44:** 170–181.

Lathrop A, MacCulloch RD. 2007. A new species of *Oreophrynella* (Anura: Bufonidae) from Mount Ayanganna, Guyana. *Herpetologica* **63:** 87–93.

MacCulloch RD, Lathrop A. 2002. Exceptional diversity of *Stefania* (Anura: Hylidae) on Mount Ayanganna, Guyana: three new species and new distribution records. *Herpetologica* **58:** 327–346.

Manzano AS, Abdala V, Herrel A. 2008. Morphology and function of the forelimb in arboreal frogs: specializations for grasping ability? *Journal of Anatomy* **213:** 296–307.

Margulies SS, Thibault KL. 2000. Infant skull and suture properties: measurements and implications for mechanisms of pediatric brain injury. *Journal of Biomechanical Engineering* **122:** 364–371.

Mayr E, Phelps Jr WH. 1967. The origin of the bird fauna of the South Venezuelan highlands. *Bulletin of the American Museum of Natural History* **136:** 269–328.

McDiarmid RW. 1971. Comparative morphology and evolution of frogs of the Neotropical genera *Atelopus*, *Dendrophryniscus*, *Melanophryniscus*, and *Oreophrynella*. *Bulletin of the Los Angeles County Museum of Natural History* **12:** 1–66.

McDiarmid RW, Donnelly MA. 2005. The herpetofauna of the Guayana Highlands: amphibians and reptiles of the Lost World. In: Donnelly MA, Crother BI, Guyer C, Wake MH,

White ME, eds. *Ecology and Evolution in the Tropics: A Herpetological Perspective*. Chicago: University of Chicago Press, pp. 461–560.

McDiarmid RW, Gorzula S. 1989. Aspects of the reproductive ecology and behavior of the tepui toads, genus *Oreophrynella* (Anura, Bufonidae). Copeia **1989(2):** 445–451.

Mendelson JRM III. 1997. The systematics of the *Bufo valliceps* group (Anura: Bufonidae) of middle America. PhD Thesis, University of Kansas, USA.

Mourthe I, Hernandez E, Señaris JC. 2017. *Oreophrynella quelchii* (Roraima Black Frog). Arboreal night shelter. Herpetological Review **48(3):** 609–610.

Noble GK. 1926. The pectoral girdle of the brachycephalid frogs. *American Museum Novitates* **230:** 1–14.

Noble DC, McKee EH, Mourier T, Mégard F. 1990. Cenozoic stratigraphy, magmatic activity, compressive deformation, and uplift in northern Peru. *Geological Society of America Bulletin* **102:** 1105–1113.

Páez-Moscoso DJ, Guayasamin JM, Yánez-Muñoz M. 2011. A new species of Andean toad (Bufonidae, *Osornophryne*) discovered using molecular and morphological data, with a taxonomic key for the genus. *ZooKeys* **108:** 73–97.

Pramuk JB. 2006. Phylogeny of South American *Bufo* (Anura: Bufonidae) inferred from combined evidence. *Zoological Journal of the Linnean Society* **146:** 407–452.

Revell LJ. 2012. phytools: An R package for phylogenetic comparative biology (and other things). *Methods in Ecology and Evolution* **3:** 217–223.

Rodrigues de Oliveira MIR, Weber LN, Napoli MF. 2014. Chondrocranial and hyobranchial morphology in larvae of the genus *Rhinella* Fitzinger, 1826 (Amphibia, Anura, Bufonidae). *Herpetological Journal* **24:** 229–236.

Salerno PE, Ron SR, Señaris JC, Rojas-Runjaic FJM, Noonan BP, Cannatella DC. 2012. Ancient Tepui summits harbor young rather than old lineages of endemic frogs. *Evolution* **66:** 3000–3013.

Señaris JC, Ayarzagüena J, Gorzula S. 1994. Los sapos de la familia Bufonidae (Amphibia: Anura) de las tierras altas de la Guyana Venezolana: descripción de un nuevo genero y tres especies. Publicaciones de la Asociación de amigos de Doñana **3:** 1–37.

Señaris JC, DoNascimiento C, Villarreal O. 2005. A new species of the genus *Oreophrynella* (Anura; Bufonidae) from the Guiana highlands. *Papéis Avulsos de Zoologia* **45:** 61–67.

Sustaita D, Pouydebat E, Manzano A, Abdala V, Hertel F, Herrel A. 2013. Getting a grip on tetrapod grasping: form, function, and evolution. *Biological Reviews* **88:** 380–405.

Trueb L. 1973. Bones, frogs, and evolution. In: Vial JL, ed. *Evolutionary Biology of the Anurans, Contemporary Research on Major Problems*. Columbia: University of Missouri Press, pp. 66–132.

Trueb L. 1993. Patterns of cranial diversity among the Lissamphibia. In: Hanken J, Hall BK, eds. *The Skull*, *Vol. 2, Patterns of Structural and Systematic Diversity*. Chicago: University of Chicago Press, pp. 255–343.

Van Bocxlaer I, Loader S, Roelants K, Biju SD, Menegon M, Bossuyt F. 2010. Gradual adaptation toward a range-expansion phenotype initiated the global radiation of toads. *Science* **327:** 679–682.

Vlassenbroeck J, Dierick M, Masschaele B, Cnudde V, Van Hoorebeeke L, Jacobs P. 2007. Software tools for quantification of X-ray microtomography at the UGCT. *Nuclear Instruments & Methods in Physics Research, Section A Accelerators, Spectrometers, Detectors, Associated Equipment* **580:** 442–445.

Wood JL. 1971. Dynamic response of human cranial bone. *Journal of Biomechanics* **4:** 1–12.

Zhou Z, Fortuny J, Marcé-Nogué J, Skutschas PP. 2017. Cranial biomechanics in basal urodeles: the Siberian salamander (*Salamandrella keyserlingii*) and its evolutionary and developmental implications. *Scientific Reports* **7:** 1–11.

Figure legends

Figure 1. Morphological diversity in *Oreophrynella*. (A) *O. huberi*, male, 18.3 mm (*O. huberi* species group), terrestrial; (B) *O. seegobini*, male, 20.0 mm (*O. weiassipuensis* species group), terrestrial; (C) *O. macconnelli*, male, 22.7 mm (*O. macconnelli* species group), arboreal; (D) *O. nigra*, female, 22.5 mm (*O. quelchii* species group), terrestrial.

Figure 2. Aerial photograph (taken on the 15th of August 2018, looking west) of the Roraima-tepui "Prow" showing summit isolation from the surrounding uplands/lowlands, and steep vertical cliffs.

Figure 3. Visual summary of the phylogenetic relationships of the main bufonid genera osteologically examined in this study. (A) dorsal view of cranium of "atelopodid" genera + *Nannophryne* on a pruned version (red branch leads to derived bufonid genera) of the Bayesian tree of Kok *et al.* (2018); (B) dorsal view of cranium of "atelopodid" genera for which molecular phylogenetic relationships remain unknown. Images not to scale.

Figure 4. Osteological characters of the axial and appendicular skeleton of *Oreophrynella quelchii* (IRSNB17139, adult female from Roraima-tepui, Guyana, 22.8 mm SVL), (A) dorsal and (B) ventral views. Cranium is in light grey and depicted in detail in Fig. 5.

Figure 5. Osteological characters of the cranium of *Oreophrynella quelchii* (IRSNB17139, adult female from Roraima-tepui, Guyana, 22.8 mm SVL), (A) dorsal, (B) ventral, and (C) lateral views.

Figure 6. Micro-CT images of the left hand of (A) *Oreophrynella quelchii* (IRSNB17140, adult female from Roraima-tepui, Guyana, 26.7 mm SVL); (B) *Oreophrynella macconnelli* (IRSNB14335, adult male from Maringma-tepui, Guyana, 22.3 mm SVL); and (C) *Atelopus hoogmoedi* (IRSNB17145, adult male from Iwokrama, Guyana, 28.3 mm SVL) in ventral view. Black rectangle highlights the difference in size and shape of the distally enlarged terminal phalanx between terrestrial (A) and arboreal (B) species of *Oreophrynella*.

Figure 7. Micro-CT images of the left foot of (A) *Oreophrynella quelchii* (IRSNB17142, adult female from Roraima-tepui, Guyana, 22.1 mm SVL); (B) *Oreophrynella macconnelli* (IRSNB14334, adult male from Maringma-tepui, Guyana, 22.2 mm SVL); and (C) *Atelopus hoogmoedi* (IRSNB17145, adult male from Iwokrama, Guyana, 28.3 mm SVL) in ventral view. Black rectangle highlights the difference in size and shape of the distally enlarged terminal phalanx between terrestrial (A) and arboreal (B) species of *Oreophrynella*.

Figure 8. Micro-CT images of the skulls of all nine species of *Oreophrynella* in dorsal view. (A) *O. nigra* (CPI10591, adult female from Kukenán-tepui, Venezuela, 22.0 mm SVL); (B) *O. quelchii* (IRSNB17139, adult female from Roraima-tepui, Guyana, 22.8 mm SVL); (C) *O. vasquezi* (IRSNB17144, adult female from Tramen-tepui, Venezuela, 23.1 mm SVL); (D) *O. macconnelli* (IRSNB14335, adult male from Maringma-tepui, Guyana, 22.3 mm SVL); (E) *O. seegobini* (IRSNB1980, adult male from Maringma-tepui, Guyana, 20.6 mm SVL); (F) *O. weiassipuensis* (CPI10901, adult male from Wei-Assipu-tepui, Guyana, 20.9 mm SVL); (G)

O. dendronastes (ROM39647, adult female from Mount Ayanganna, Guyana, 33.2 mm SVL); (H) *O. huberi* (IRSNB17135, adult male from Cerro El Sol, Venezuela, 19.2 mm SVL); and (I) *O. cryptica* (IRSNB17134, adult male from Auyán-tepui, Venezuela, 22.8 mm SVL). Scale bars = 2 mm.

Figure 9. Micro-CT images of the skulls of all nine species of *Oreophrynella* in ventral view. (A) *O. nigra* (CPI10591, adult female from Kukenán-tepui, Venezuela, 22.0 mm SVL); (B) *O. quelchii* (IRSNB17139, adult female from Roraima-tepui, Guyana, 22.8 mm SVL); (C) *O. vasquezi* (IRSNB17144, adult female from Tramen-tepui, Venezuela, 23.1 mm SVL); (D) *O. macconnelli* (IRSNB14335, adult male from Maringma-tepui, Guyana, 22.3 mm SVL); (E) *O. seegobini* (IRSNB1980, adult male from Maringma-tepui, Guyana, 20.6 mm SVL); (F) *O. weiassipuensis* (CPI10901, adult male from Wei-Assipu-tepui, Guyana, 20.9 mm SVL); (G) *O. dendronastes* (ROM39647, adult female from Mount Ayanganna, Guyana, 33.2 mm SVL), (H) *O. huberi* (IRSNB17135, adult male from Cerro El Sol, Venezuela, 19.2 mm SVL); and (I) *O. cryptica* (IRSNB17134, adult male from Auyán-tepui, Venezuela, 22.8 mm SVL). Scale bars = 2 mm.

Figure 10. Micro-CT images of the skulls of all nine species of *Oreophrynella* in lateral view. (A) *O. nigra* (CPI10591, adult female from Kukenán-tepui, Venezuela, 22.0 mm SVL); (B) *O. quelchii* (IRSNB17139, adult female from Roraima-tepui, Guyana, 22.8 mm SVL); (C) *O. vasquezi* (IRSNB17144, adult female from Tramen-tepui, Venezuela, 23.1 mm SVL); (D) *O. macconnelli* (IRSNB14335, adult male from Maringma-tepui, Guyana, 22.3 mm SVL); (E) *O. seegobini* (IRSNB1980, adult male from Maringma-tepui, Guyana, 20.6 mm SVL); (F) *O. weiassipuensis* (CPI10901, adult male from Wei-Assipu-tepui, Guyana, 20.9 mm SVL),, (G) *O. dendronastes* (ROM39647, adult female from Mount Ayanganna, Guyana, 33.2 mm SVL),

(H) *O. huberi* (IRSNB17135, adult male from Cerro El Sol, Venezuela, 19.2 mm SVL), and (I) *O. cryptica* (IRSNB17134, adult male from Auyán-tepui, Venezuela, 22.8 mm SVL). Scale bars = 2 mm.

Figure 11. Hypothetical evolution of (A) arboreality, (B) zygodactyly, (C) condition of parietal and frontoparietal fontanelles, and (D) condition of presacral vertebrae in "atelopodid" Bufonidae + *Nannophryne*, summarized from 1,000 iterations of stochastic character mapping across the timetree of Kok *et al.* (2018) and summarized at each node. Branches coloured in red and red arrows indicate assumed dispersal to Pantepui (Kok *et al.*, 2018).

Table 1. Specimens used for the osteological analysis**.** Museum acronyms: CPI, Coastal Plains Institute and Land Conservancy (Florida, USA); ROM, Royal Ontario Museum (Ontario, Canada); IRSNB, Institut Royal des Sciences Naturelles de Belgique (Brussels, Belgium); USNM, United States National Museum (Washington, USA); ZUEC, Museu de Zoologia da Universidade Estadual de Campinas (São Paulo, Brazil). Abbreviations: M, male; F, female; JUV, juvenile.

Species	Catalogue number	Locality	Sex
Oreophrynella cryptica	IRSNB17131	Auyán-tepui, Venezuela	M
Oreophrynella cryptica	IRSNB17132	Auyán-tepui, Venezuela	M
Oreophrynella cryptica	IRSNB17133	Auyán-tepui, Venezuela	F
Oreophrynella cryptica	IRSNB17134	Auyán-tepui, Venezuela	M
Oreophrynella dendronastes	ROM39647	Mount Ayanganna, Guyana	F
Oreophrynella huberi	IRSNB17135	Cerro el Sol, Venezuela	M
Oreophrynella huberi	IRSNB17136	Cerro el Sol, Venezuela	M
Oreophrynella macconnelli	IRSNB14334	Maringma-tepui, Guyana	M
Oreophrynella macconnelli	IRSNB14335	Maringma-tepui, Guyana	M
Oreophrynella macconnelli	IRSNB14364	Roraima-tepui, Guyana	F
Oreophrynella macconnelli	CPI10725	Wei-Assipu-tepui, Guyana	M
Oreophrynella nigra	IRSNB15732	Yuruaní-tepui, Venezuela	F
Oreophrynella nigra	IRSNB17138	Yuruaní-tepui, Venezuela	F
Oreophrynella nigra	IRSNB17137	Kukenán-tepui, Venezuela	M
Oreophrynella nigra	IRSNB14383	Kukenán-tepui, Venezuela	M
Oreophrynella nigra	IRSNB14388	Kukenán-tepui, Venezuela	F
Oreophrynella quelchii	IRSNB15866	Wei-Assipu-tepui, Guyana	M
Oreophrynella quelchii	IRSNB17139	Roraima-tepui, Guyana	F
Oreophrynella quelchii	IRSNB17140	Roraima-tepui, Guyana	F
Oreophrynella quelchii	IRSNB17141	Roraima-tepui, Guyana	M
Oreophrynella quelchii	IRSNB17142	Roraima-tepui, Guyana	F
Oreophrynella seegobini	IRSNB1979	Maringma-tepui, Guyana	M
Oreophrynella seegobini	IRSNB1980	Maringma-tepui, Guyana	M
Oreophrynella vasquezi	IRSNB15761	Tramen-tepui, Venezuela	M
Oreophrynella vasquezi	IRSNB17143	Tramen-tepui, Venezuela	F
Oreophrynella vasquezi	IRSNB17144	Tramen-tepui, Venezuela	F
Oreophrynella vasquezi	IRSNB14393	Ilú-tepui, Venezuela	F
Oreophrynella vasquezi	IRSNB14395	Ilú-tepui, Venezuela	F
Oreophrynella weiassipuensis	CPI10901	Wei-Assipu-tepui, Guyana	M
Oreophrynella weiassipuensis	CPI10902	Wei-Assipu-tepui, Guyana	F
Amazophrynella manaos	IRSNB15817	Iwokrama, Guyana	F
Atelopus hoogmoedi	IRSNB17145	Iwokrama, Guyana	M
Atelopus ignescens	IRSNB425.C	No precise locality, Ecuador	M
Dendrophryniscus brevipollicatus	IRSNB57.C	São Paolo, Brazil	F
Frostius erythrophthalmus	ZUEC16631	Bahia state, Brazil	F
Melanophryniscus moreirae	USNM207760	No precise locality, Brazil	F
Metaphryniscus sosai	USNM550143	Marahuaka-tepui, Venezuela	F
Undescribed bufonid	USNM562237	La Neblina, Venezuela	F
Undescribed bufonid	USNM562238	La Neblina, Venezuela	F
Undescribed bufonid	USNM562242	La Neblina, Venezuela	F
Undescribed bufonid	USNM562248	La Neblina, Venezuela	M
Undescribed bufonid	USNM562249	La Neblina, Venezuela	M
Undescribed bufonid	USNM562255	La Neblina, Venezuela	M
Nannophryne variegata	IRSNB12826	Villarrica National Park, Chile	F
Osornophryne bufoniformis	USNM193540	Napo province, Ecuador	F
Rhaebo guttatus	IRSNB17146	Iwokrama, Guyana	JUV
Rhinella beebei	IRSNB17147	Kamarata, Venezuela	F

Table 2. Taxa by character matrix used for the osteological comparisons (mostly based on Pramuk 2006). * = data from Pramuk (2006); NA = not applicable; - = not available; ? = unknown

Taxon	1	2	3	4	5	6	7	8	9	10	11	12	13	14	15	16	17	18	19	20	21	22	23	24	25	26	27	28
Oreophrynella nigra	0	0	0	0	0	0/1	0	0	0	1	1	0	1	0	1	1	NA	0	0	2	0	1	0	0	0	0	1	1
Oreophrynella quelchii	0	0	0	0	0	0/1	0	0	0	1	1	0	1	0	1	1	NA	0	0	2	0	1	0	0	0	0	1	1
Oreophrynella vasquezi	0	0	0	0	0	0/1	0	0	0	1	1	0	1	0	1	1	NA	0	0	2	0	1	0	0	0	0	1	1
Oreophrynella seegobini	1	0	0	0	0	1	0	0	0	1	1	0	2	0	1	1	NA	0	0	0/2	0	1	2	0	0	0	1	1
Oreophrynella weiassipuensis	1	0	0	0	0	1	0	0	0	1	0/1	0	2/3	0/1	1	1	NA	0	0	0/2	0	1	2	0	0	0	1	1
Oreophrynella macconnelli	0	0	0	0	0	0/1	0	0	0	1	1	0	1	0	1	1	NA	0	0	0/2	0	1	2	0	0	0/1	1	1
Oreophrynella dendronastes	0	0	0	0	0	0	0	0	0	1	1	0	1	0	1	1	NA	0	0	2	0	1	2	0	0	0/1	1	1
Oreophrynella cryptica	0	1	0	0	1	1	0	0	0	1	1	0	3	1	1	1	NA	0/1	0	0/2	0	1	2	0/1	0	0/1	1	1
Oreophrynella huberi	0	1	0	0	1	1	0	0	0	1	1	0	3	1	1	1	NA	0/1	0	0/2	0	1	2	0/1	0	1	1	1
Atelopus manaos	0	0	0	0	0	1	0	0	1	0	0	0	1	0	1	1	NA	0	0	2	0	1	2	0	0	1	0	1
Atelopus hoogmoedi	0	0	0	0	0	2	1	0/1	0	0	0	0	0	0	1	0	0	0	0	0	0	1	2	2	0	1	1	2
Atelopus ignescens	0	0	0	0	0	2	1	0	0	0	0	0	0	0	1	1	NA	0	0	0	0	1	0	0	0	1	1	2
Dendrophryniscus brevipollicatus	0	1	0	0	0	0	0/1	0/3	1	0	0	1	0	1	1	NA	0	0	0	0	0	1	2	0	0	1	0	2
Frostius erythrophthalmus	2	0/1	0	0	1	2	0	0	0	0	0	0	0	2	1	0	0	0	0	0	0	0	2	0	1	1	1	1
*Melanophryniscus**	0	1	0	0	2	0	-	0	0	-	-	0	-	0	1	1	NA	0	0	0	0	1	0	0	-	1	0	2
Melanophryniscus moreirae	0	1	0	0	2	0/1	1	0	0	0	0	0	0	0	1	1	NA	0	0	0	0	0	0	0	0	?	0	2
Metaphryniscus sosai	0	0	0	0	0	2	0	0	0	0	0	0	1	0	1	1	NA	1	0	0	1	1	0	0	0	1	1	1
*Nannophryne cophotis**	0	0	0	0	0	0	-	2	0	-	-	0	-	0	1	1	NA	0	0	2	0	1	1	0	-	1	1	1
*Nannophryne corynetes**	0	1	0	0	0	0	-	1	0	-	-	0	-	0	1	1	NA	0	0	2	0	1	0	0	-	1	1	1
*Nannophryne variegata**	0	1	0	0	0	0	-	2	0	-	-	0	-	0	1	1	NA	0	0	2	0	1	0	0	-	0	1	1
Nannophryne variegata	0	1	0	0	0	0	0	0	0	0	0	0	1	0	0/1	1	NA	0	0	2	0	0	0	0	0	0	0	1
*Osornophryne**	1	0	0	0	0	2	-	1	0	-	-	0	-	0	1	1	NA	1	0	0	0	0	0	2	-	1	2	0
Osornophryne bufoniformis	2	0	0	0	0	?	0/1	0	1	0	0	0	0	0	1	1	NA	0	0	0	0	0	0	0	1	1	1/2	1
*Rhinella granulosa/humboldti**	2	0	0	0	2	2	-	2	0	-	-	0	-	2	1	0	0	2	0	?	0	?	2	2	-	0	2	2/1
Rhinella beebei	2	1	0	0	2	2	0	1	0	0	0	0	2/3	2	1	0	0	2	0	?	0	0	2	0	0	0	2	1
*Rhaebo guttatus**	1	0	0	0	0	2	-	2	0	-	-	0	-	0	1	0	0	1	1	0	0	0	0	0	-	0	2	0
*Truebella skoptes**	0	0	1	1	0	2	-	1	1	-	-	0	-	0	1	1	NA	0	0	0	0	1	0	0	-	1	0	1
Truebella skoptes	0	0	0/1	0	0	0	0	0	0/1	0	0	0	1	0	1	1	NA	0	0	2	0	1	0	0	0	1	1	1
*Truebella tothastes**	0	0	1	1	0	2	-	1	1	-	-	0	-	0	1	1	NA	0	0	0	0	1	0	0	-	1	0	1
Truebella tothastes	0	0	0	0	0	0	0	0	1	0	0	0	1	0	1	1	NA	0	0	2	0	1	0	0	0	1	0	1
New bufonid	0/1	0/1	0	0	0	2	0/1	0	0/1	0	0	0	2/3	0/1	1	1	NA	0/1	0	0	0/1	1	2	0	0	1	1	1

Table 2 (Continued). Taxa by character matrix used for the osteological comparisons (mostly based on Pramuk 2006). * = data from Pramuk (2006); NA = not applicable; - = not available; ? = unknown

Taxon	29	30	31	32	33	34	35	36	37	38	39	40	41	42	43	44	45	46	47	48	49	50	51	52	53	54	55	56
Oreophrynella nigra	1	0	1	0	3	3	1	-	-	-	-	2	1	2	1	1	0	0	0	2	0	0	0	0	1	0	1	0
Oreophrynella quelchii	1	0	1	0	3	3	1	-	-	-	-	2	1	2	1	1	0	0	0	2	0	0	0	0	1	0	1	0
Oreophrynella vasquezi	1	0	1	0	3	3	1	-	-	-	-	2	1	2	1	1	0	0	0	2	0	0	0	0	1	0	1	0
Oreophrynella seegobini	1	0	1	0	3	3	1	-	-	-	-	2	1	2	1	1	0	0	0	2	0	0	0	1	1	0	1	0
Oreophrynella weiassipuensis	1	0	1	0	3	3	1	-	-	-	-	2	1	2	1	1	0	0	0	2	0	0	0	1	1	0	1	0
Oreophrynella macconnelli	NA	NA	NA	0	3	3	1	-	-	-	-	2	1	2	1	1	0	0	0	2	0	0	0	0	1	0	1	0
Oreophrynella dendronastes	NA	NA	NA	0	3	3	1	-	-	-	-	2	1	2	1	1	0	0	0	2	0	0	0	0	1	0	1	0
Oreophrynella cryptica	1	0	1	0	3	3	1	-	-	-	-	2	1	2	1	1	0	0	0	2	1	1	0	1	1	1	1	0
Oreophrynella huberi	1	0	1	0	3	3	1	-	-	-	-	2	1	2	1	1	0	0	0	2	1	1	0	1	1	1	1	0
Atelopus manaos	1	1	1	0	3	0	0	0	0/1	1	1/2	0/1	1	2	1	1	0	0	0	2	0	0	0	0	0	0	0	0
Atelopus hoogmoedi	1	0	1	0	3	1	1	1	1	1	-	1	1	1	1	0/1	1	1	1	2	0	0	0	0	0	0	0	1
Atelopus ignescens	1	0	1	0	3	1	1	1	1	1	-	1	1	2	1	0/1	0	0	1	2	0	0	0	0	0	0	0	0
Dendrophryniscus brevipollicatus	1	?	?	0	3	?	0/1	1	2	-	-	1	1	2	1	1	1	0	0/1	2	0	0	0	0	0	0	0	0
Frostius erythrophthalmus	1	0	1	0	0	0	0	0/1	0	1	2	1	1	2	1	1	0	0	0	2	0	?	0	1	0	0	0/1	1
*Melanophryniscus**	1	0	0	0	0	0	-	0	1	2	1	1	0	2	1	0	-	-	-	2	0	0	0	0	0	0	0	0
Melanophryniscus moreirae	1	?/0	?	0	3	0	0	0	1	1/2	2	0	0	2	1	0	0	0	0	2	0	0	0	0	0	0	0	0
Metaphryniscus sosai	1	1	0/1	0	2	2	0	0	2	-	-	2	1	2	1	0	0	0	0/1	2	0	0	0	0	0	0/1	0	0
*Nannophryne cophotis**	0	0	1	0	0	0	-	1	0	2	1	0	0	2	1	0	-	-	-	1	1	0	0	0	0	0	0	0
*Nannophryne corynetes**	0	1	1	0	3	0	-	1	1	2	1	0	1	2	1	0	-	-	-	1	1	0	0	0	0	0	0	0
*Nannophryne variegata**	1	0	1	0	3	0	-	1	0	2	1	0	1	2	1	0	-	-	-	1	1	0	0	0	0	0	0	0
Nannophryne variegata	1	0	1	0	3	0	0	1	1/2	2	2	0	0/1	2	1	0	0	0	0	0/1	0/1	0	0	0	0	0	0	0
*Osornophryne**	1	?	1	0	2	<8	-	?	?	?	?	2	1	2	1	0	-	-	-	2	1	0	0	0	0	0	0	0
Osornophryne bufoniformis	1	?/1	1	0	3	2	0	1	1	-	-	2	1	2	1	0	0	2	1	2	0/1	?	0	0/1	0	0	0/1	0
*Rhinella granulosa/humboldti**	0	0	0	1	?	0	-	0	0	2	1	1	1	2	1	0	-	-	-	?/0/2	1	1	1	1	1	1	1	1
Rhinella beebei	0	0	0	1	?	0	0	0	0	2	1/2	0	0	2	1	0	0	0	0	?	1	?	1	1	1	1	1	1
*Rhaebo guttatus**	0	0	1	0	0	0	-	2	0	2	1	1	0	1	0	0	-	-	-	0	1	1	0	0	0	1	1	1
*Truebella skoptes**	0	0	1	0	3	<8	-	1	0	0	?	0	1	2	1	0	-	-	-	2	0	0	0	0	0	0	0	0
Truebella skoptes	1	0	1	0	3	0	0	0	0	1	2	0	1	2	1	1	0	0	0/1	2	0	0	0	0	0	0	0	0
*Truebella tothastes**	0	0	1	0	3	0	-	1	1	2	1	0	1	2	1	0	-	-	-	2	0	0	0	0	0	0	0	0
Truebella tothastes	1	0	1	0	3	0	0	0	1	1/2	2	1	1	2	1	1	0	0	0/1	2	0	0	0	0	0	0	0	0
New bufonid	1	1	1	0	2	3	1	-	-	-	-	2	1	2	1	1	0	0	0	2	0	1	0	0/1	0	0/1	0/1	0

Appendix 1. Morphological character descriptions (modified from Pramuk, 2006)**.** Each account provides a description of the different character states and their coding:

1. Sculpturing of dermal roofing bones. The dermal bones (i.e. frontoparietals, sphenethmoid, and nasals) display varying degrees of ornamentation that result from exostosis. Dermal bones of skull completely smooth (0); lightly exostosed (1); heavily ornamented with pits, striations, and/or rugosities (2).
2. Medial contact of nasals. The nasal bones may contact along their entire length, or as in some lightly ossified species may be separated medially. Nasals not contacting medially (0); medial contact present (1).
3. Shape of anterior margins of nasals. In dorsal view, the shape of the anterior margin of the paired nasal bones is variable. The shape of the anterior margins can be relatively blunt (0); or acuminate (1).
4. Shape of posterior margins of nasals. In dorsal view, the shape of the posterior margin of the nasal bones is variable. The posterior margins may be arcuate (0); relatively blunt and perpendicular to the medial axis of the skull (1); or extremely arcuate (2).
5. Contact between nasals and frontoparietal. No contact between nasals and frontoparietal, dorsal surface of sphenethmoid visible (0); contact between nasals and frontoparietal, dorsal surface of sphenethmoid visible (1); contact between nasals and frontoparietal, dorsal surface of sphenethmoid not visible (2).
6. Occipital artery pathway. The groove encloses the occipital artery and lies over the prootic; the artery may be partially or entirely closed. Occipital groove uncovered (0); partially covered (1); completely covered with bone (2).
7. Contact of vomer (= prechoanal vomer) with sphenethmoid. Vomer not contacting sphenethmoid (0); vomer contacting sphenethmoid. (1).
8. Contact of anterior process of vomer and maxilla. The anterior process of vomer free (0); contacting maxilla only (1); contacting maxilla and premaxilla (2); contacting premaxilla only (3).
9. Medial contact of frontoparietals. Frontoparietals in contact medially (0); separated medially (1).
10. Frontoparietal fontanelle. Frontoparietal fontanelle absent (0); present (1).
11. Parietal fontanelles. Parietal fontanelles absent (0); present (1).
12. Expansion of posterior ramus of pterygoid. Posterior ramus not expanded (0); posterior ramus expanded (1).
13. Expansion of zygomatic ramus of squamosal. Zygomatic ramus not expanded (0); slightly expanded (1); greatly expanded (2); zygomatic ramus in contact with maxilla (3).
14. Contact of zygomatic and ventral rami of squamosal. Zygomatic ramus of the squamosal free from ventral ramus and maxilla (0); zygomatic ramus of the squamosal free from ventral ramus but contacting maxilla (1); zygomatic ramus of the squamosal in contact with ventral ramus and maxilla (2).
15. Angle of the ventral ramus of the squamosal in posterior view. Ventral ramus of the squamosal angled ventrolaterally (0); ventral ramus of the squamosal approximately perpendicular to the dorsal surface of the otic capsule (1).
16. Columella (stapes). Columella present (0); absent (1).
17. Columella shape. The Columella of most anurans is a simple, rod-shaped bone. Columella is rod-shaped (0); blade-shaped and compressed anteroposteriorly (1).
18. Contact of medial ramus of pterygoid with alae of parasphenoid. The medial ramus of the pterygoid is not in contact or barely in contact with the anterolateral margin of the alae of the parasphenoid (0); fused with the anterolateral margin of the parasphenoid (1); fused and extending medially along approximately half the length of the parasphenoid alae (2).

19. Jugular foramina. In ventral view, the jugular foramina are round openings located on the ventral surface of the exoccipital (0); jugular foramina are oriented posterolaterally and are not visible in ventral view (1).
20. Anterior margins of nasals. In lateral view, the anterior margins of the nasal bones are flush with the dorsal margins of the alary processes of the premaxillae (0); extend beyond the dorsal margins of the alary processes (1); lie posterior to the dorsal margins of the alary processes (2).
21. Maxillary extension. No overlap of premaxilla by maxilla (0); maxillae extending beyond lateral margin of premaxillae (1); maxillae extending beyond half of the premaxillae (2).
22. Expansion of the pars facialis of maxilla. The pars facialis of the maxilla is a dorsally directed flange. The dorsal process is relatively expanded at the point where it contacts anteromedially with the premaxilla (0); the dorsal process is relatively equal in height from the anterior margin of the orbit to the point of contact between the maxilla and the premaxilla (1).
23. Alary process. The alary processes of the premaxillae project dorsally from the pars palatine of the premaxillae. Alary processes are perpendicular to the margin of the premaxillae (0); angled posteriorly (1); angled anteriorly (2).
24. Ridges on cultriform process of parasphenoid. The ventral surface of the cultriform process is smooth (0); ventral surface of the cultriform process bears medial ridge that is parallel to the medial axis of the skull (1); ventral surface of cultriform process bears a pair of ridges that are parallel to the medial axis of the skull (2).
25. Exostosis on medial surface of parasphenoid, at the base of the cultriform process. Surface is smooth (0); surface is exostosed (1).
26. Parasphenoid, shape of cultriform process. The cultriform is broad posteriorly and narrow and acute anteriorly (0); narrow posteriorly, broad medially, and broadly rounded, with or without acute tip anteriorly (1).
27. Direction of parasphenoid alae. The orientation of the long axes of the parasphenoid alae are posterolateral (0); lateral (1); anterolateral (2).
28. Anterior extension of the sphenethmoid. In ventral view, the anterior margin of the sphenethmoid extends anteriorly only to the posterior margin of the vomers (0); extends anteriorly approximately to the middle of the vomers (1); extends to the posterior margin of the premaxillae (2).
29. Ventral ridge of neopalatine. Ventral, transverse ridge on neopalatine present (0); ventral, transverse ridge absent (1).
30. Neopalatine, relative width medial and lateral edge. The lateral end of the neopalatine is broader than the medial end (0); the neopalatine is approximately the same width along its entire length (1); the medial end is broader than the lateral end (2).
31. Neopalatine separation. The neopalatines are nearly in contact at the midline of the sphenethmoid (0); the neopalatines are separated widely, contacting the sphenethmoid only marginally (1).
32. Prenasal bones. Prenasal bones absent (0); present (1).
33. Contact of maxilla and quadratojugal. In lateral view, the contact of the posterior margin of the maxilla with the quadratojugal may have one of three orientations: posterior edge of the maxilla positioned ventrally to the quadratojugal (0); maxilla lateral to the quadratojugal (1); maxilla positioned dorsally to the quadratojugal (2); quadratojugal reduced or absent and not in contact with the maxilla (3).
34. Number of presacral vertebrae. Eight presacral vertebrae present (0); seven presacral vertebrae present (1); six presacral vertebrae present (2); five presacral vertebrae present (3).

35. Condition of vertebrae I and II. Not fused (atlas separate from first trunk vertebra) (0); fused (atlas complex) (1).
36. Relative lengths of transverse processes of presacral vertebrae V and VI. The length of the transverse process of vertebra VI is less than the length of vertebra V (0); the length of the transverse processes of vertebrae V and VI is approximately equal (1); the length of the transverse process of vertebra VI is greater than the length of vertebra V (2).
37. Presacral vertebrae, orientation of transverse processes of presacral vertebra VI. The transverse processes of vertebra VI are orientated posterolaterally (0); perpendicular to the medial axis of the vertebral column (1); orientated anterolaterally (2).
38. Orientation of transverse processes of presacral vertebra VII. The transverse processes of vertebra VII are orientated posterolaterally (0); perpendicular to the medial axis of the vertebral column (1); orientated anterolaterally (2).
39. Orientation of transverse processes of presacral vertebra VIII. The transverse processes of vertebra VIII are orientated posterolaterally (0); perpendicular to the medial axis of the vertebral column (1); orientated anterolaterally (2).
40. Lateral flanges of urostyle. The urostyle lacks lateral flanges (0); lateral flanges present (1); flanges greatly expanded (2).
41. Shape of sacral diapophyses. The sacral diapophyses of some taxa are relatively cylindrical, whereas those of other taxa are broadly dilated and flat. The width of the sacral diapophyses is smaller than its length (0); the width is equal to, or greater than, its length (1).
42. Angle of anterior edge of sacral diapophyses. The anterior edge of the sacral diapophyses is angled approximately posteriorly (0); perpendicular to the medial axis of the vertebral column (1); angled anteriorly (2).
43. Omosternum. The omosternum is a prezonal element of the pectoral girdle. The presence of this element is homoplastic among anurans. Omosternum present (0); omosternum absent (1).
44. Shape of ultimate phalanx of manus. Ultimate phalanx of the manual digits pointed (0); ultimate phalanx of the manual digits modified T-shape (1).
45. Phalangeal formula of hand. Ancestral formula, 2-2-3-3 (0); 1-2-3-3 (1).
46. Phalangeal formula of foot. Ancestral formula, 2-2-3-4-3 (0); 1-2-3-4-3 (1); 2-2-3-4-2 (2).
47. Reduction of pollex. Normal condition (0); reduced size of phalanges (1).
48. Relative length of fingers. Length of Finger I>II (0); Finger I=II (1); Finger I<II (2).
49. Canthal crest. The terminology used for cranial crests follows Mendelson (1997). The canthal crest is formed by a raised ridge of bone along the anterolateral margin of the nasal. Absent (0); present (1).
50. Parietal crest. The parietal crest is on the frontoparietal and prootic/squamosal. Absent (0); present (1).
51. Preorbital crest. The preorbital crest is located on the maxillary process of the nasal. Absent (0); present (1).
52. Pretympanic/postorbital crests. These crests are located on the squamosal. Absent (0); present (1).
53. Suborbital crest. The suborbital crest is located on the pars facialis of the maxilla. Absent (0); present (1).
54. Supraorbital crest. Absent (0); present (1).
55. Supratympanic crest. The supratympanic crest is located on the otic ramus of the squamosal. Absent (0); present (1).
56. Supraorbital flange on frontoparietals. In ventral view, the frontoparietal extends laterally beyond the lateral margin of the sphenethmoid. Supraorbital flange absent (0); present (1).

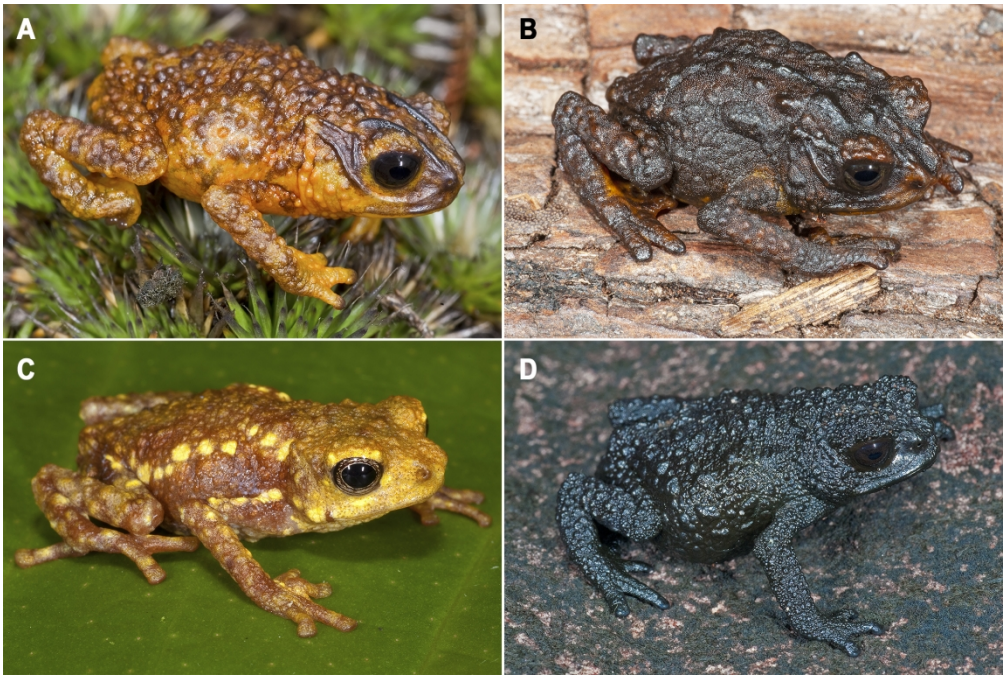

Figure 1

199x134mm (300 x 300 DPI)

Figure 2

199x149mm (300 x 300 DPI)

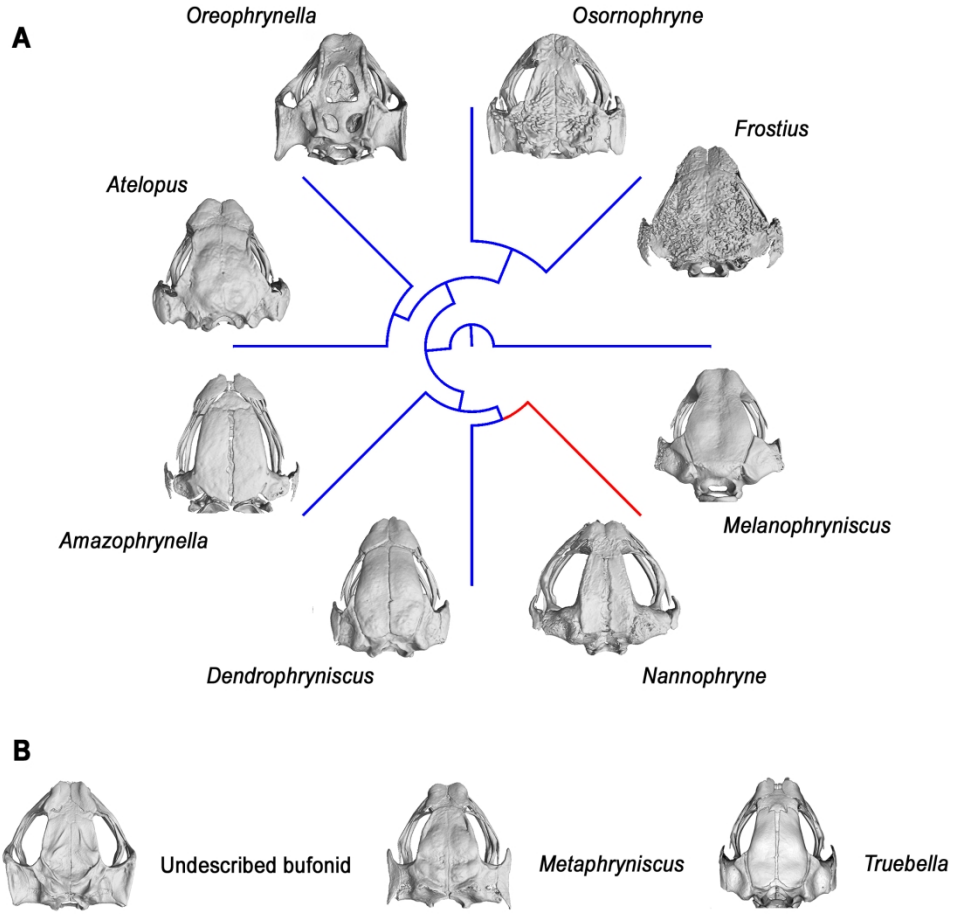

Figure 3

199x188mm (300 x 300 DPI)

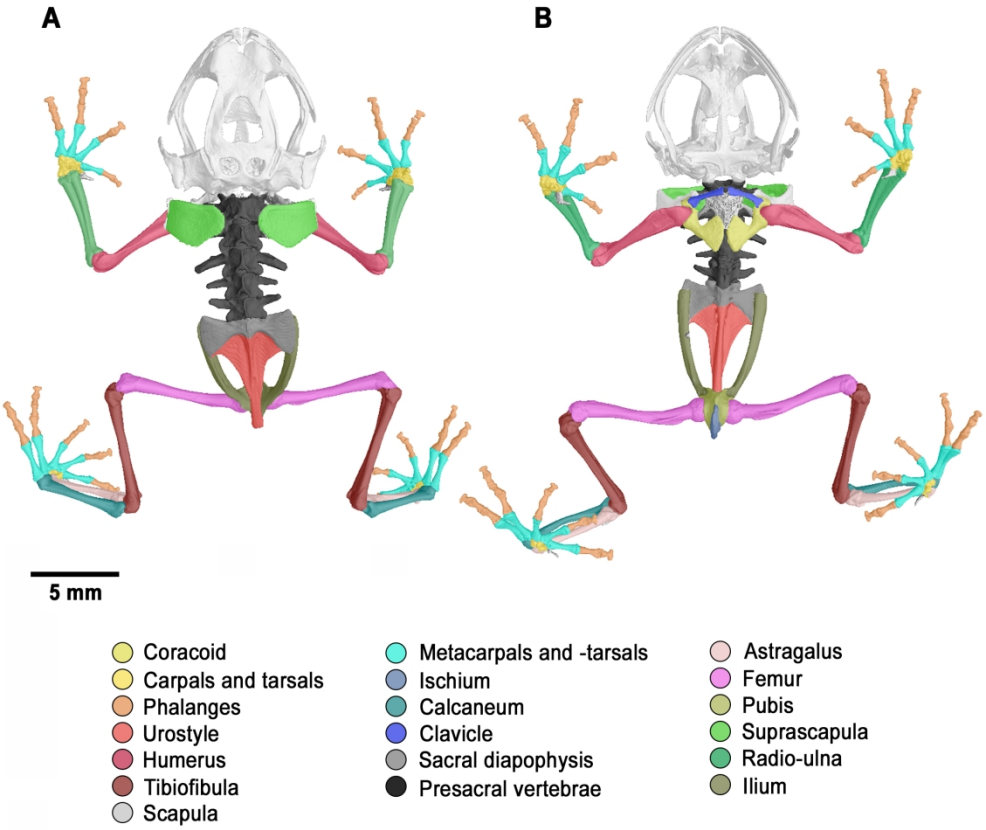

Figure 4

199x184mm (300 x 300 DPI)

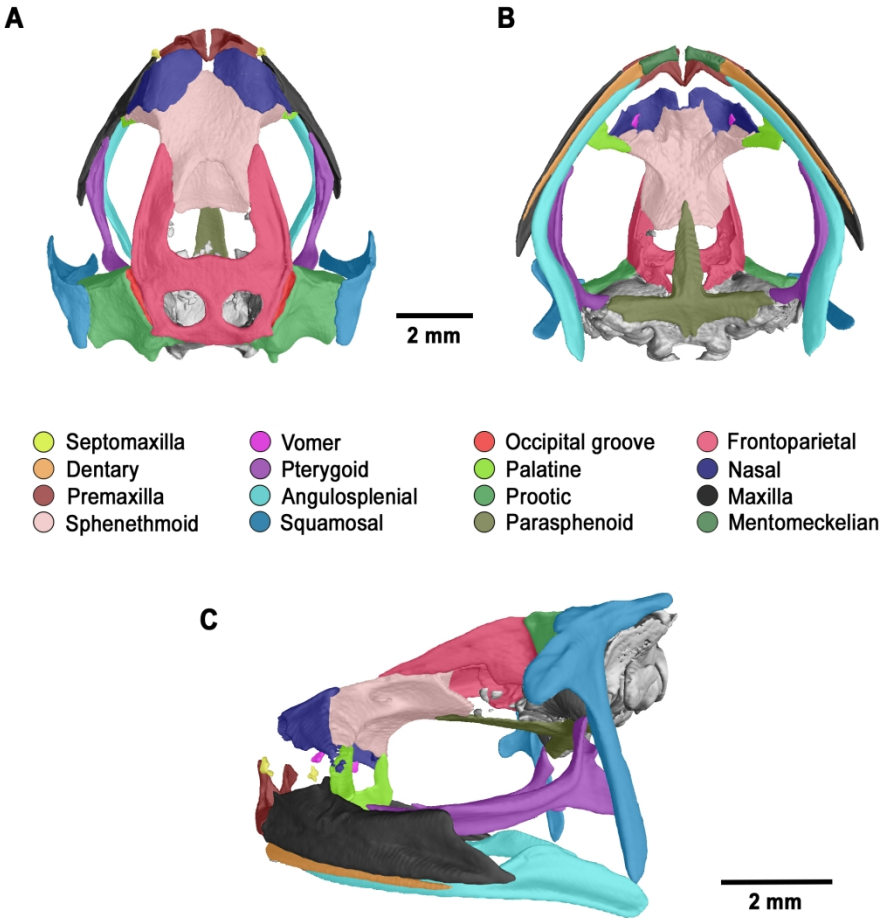

Figure 5

199x199mm (300 x 300 DPI)

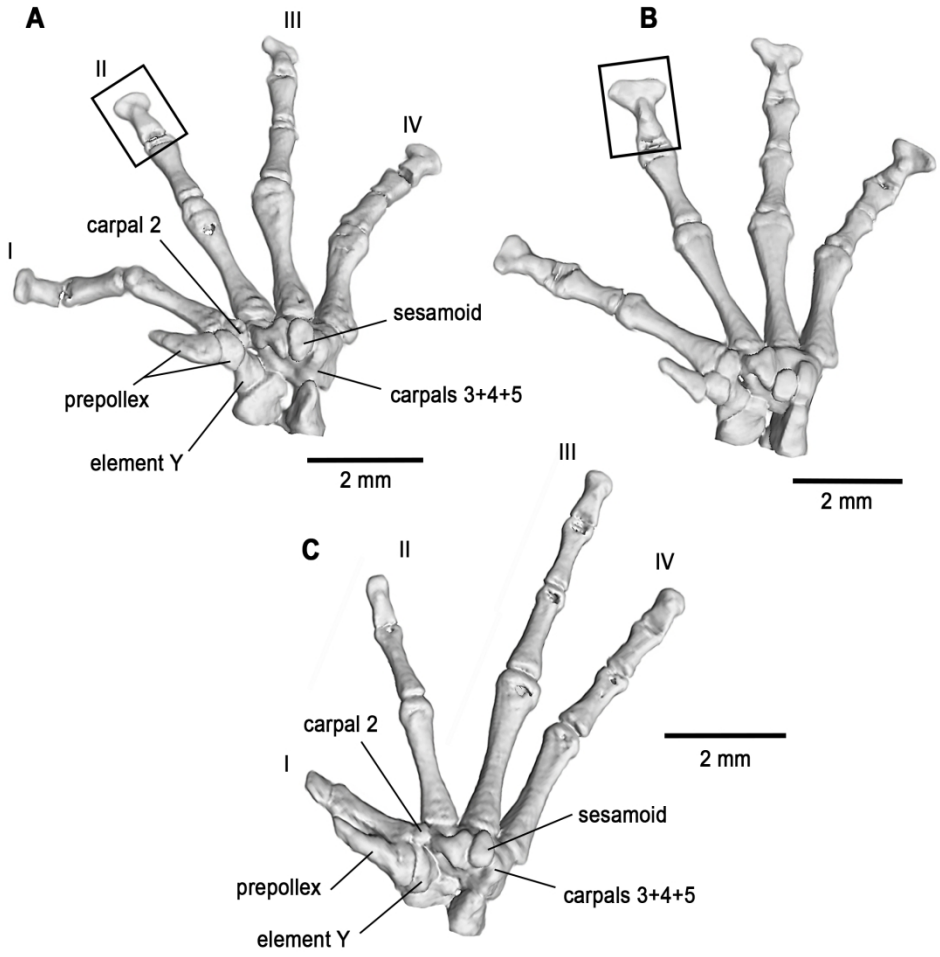

Figure 6

199x199mm (300 x 300 DPI)

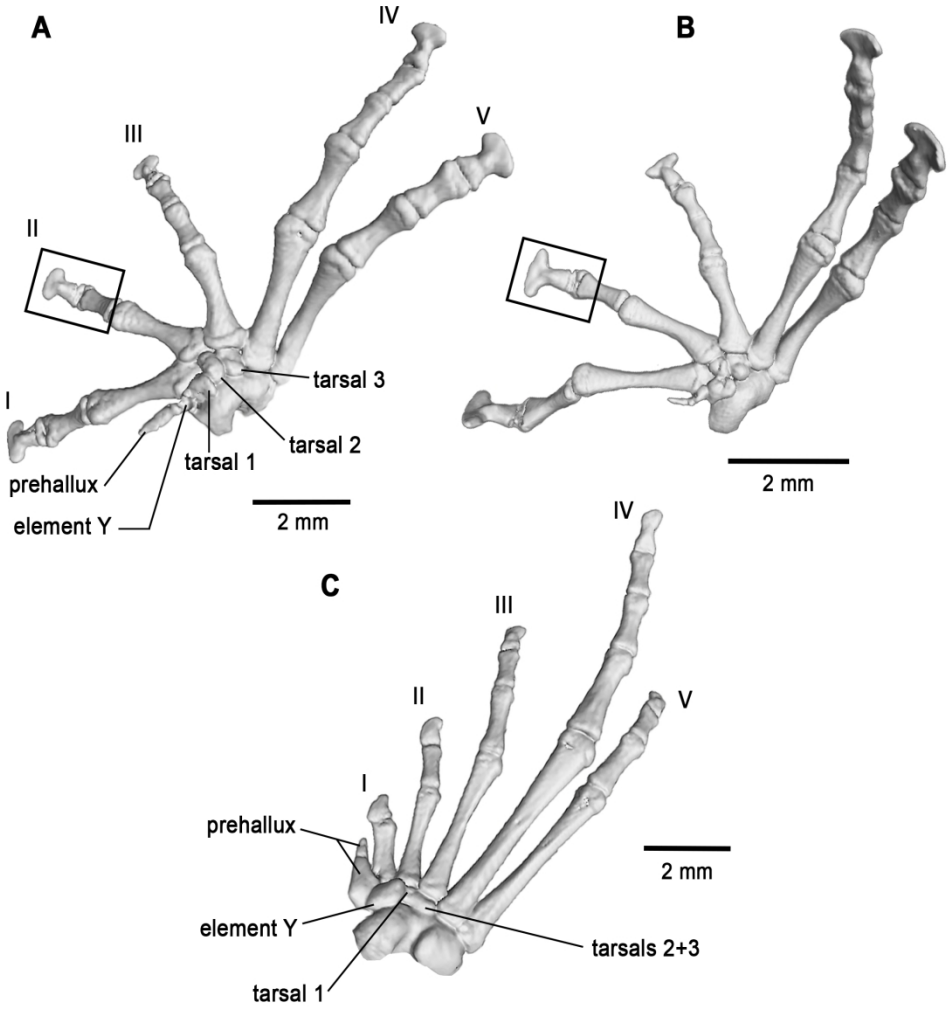

Figure 7

199x210mm (300 x 300 DPI)

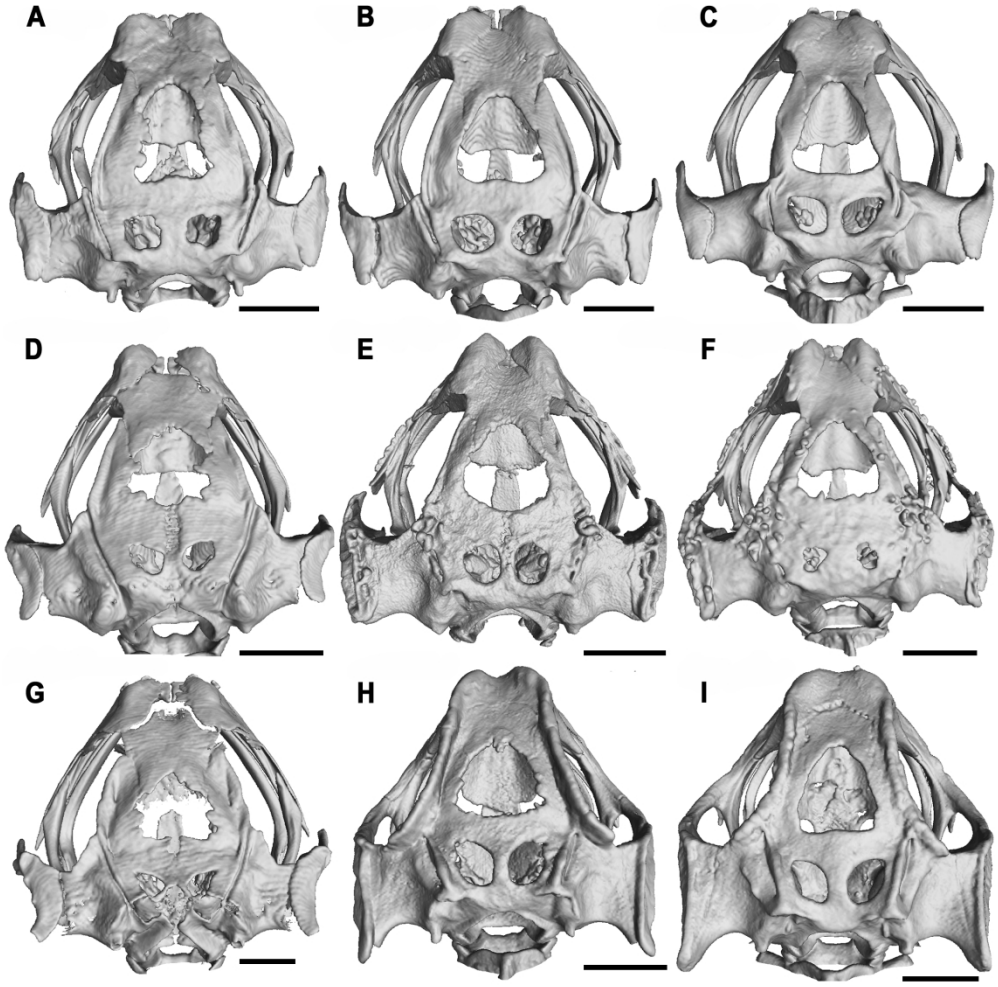

Figure 8

199x199mm (300 x 300 DPI)

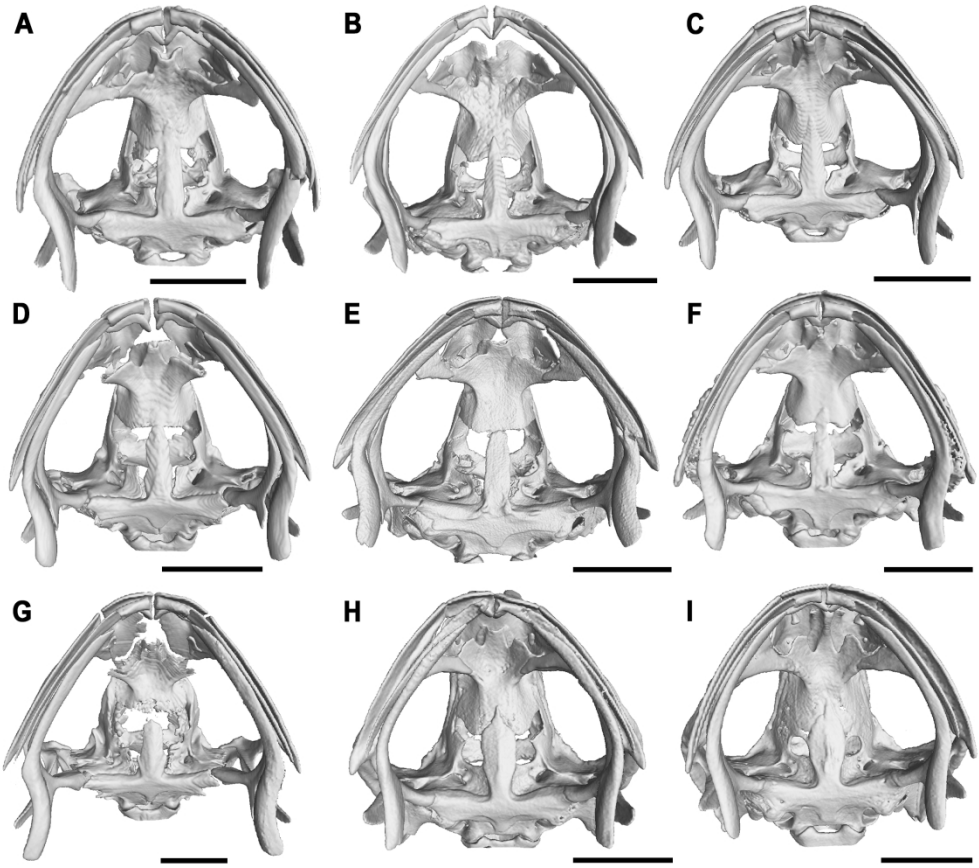

Figure 9

199x176mm (300 x 300 DPI)

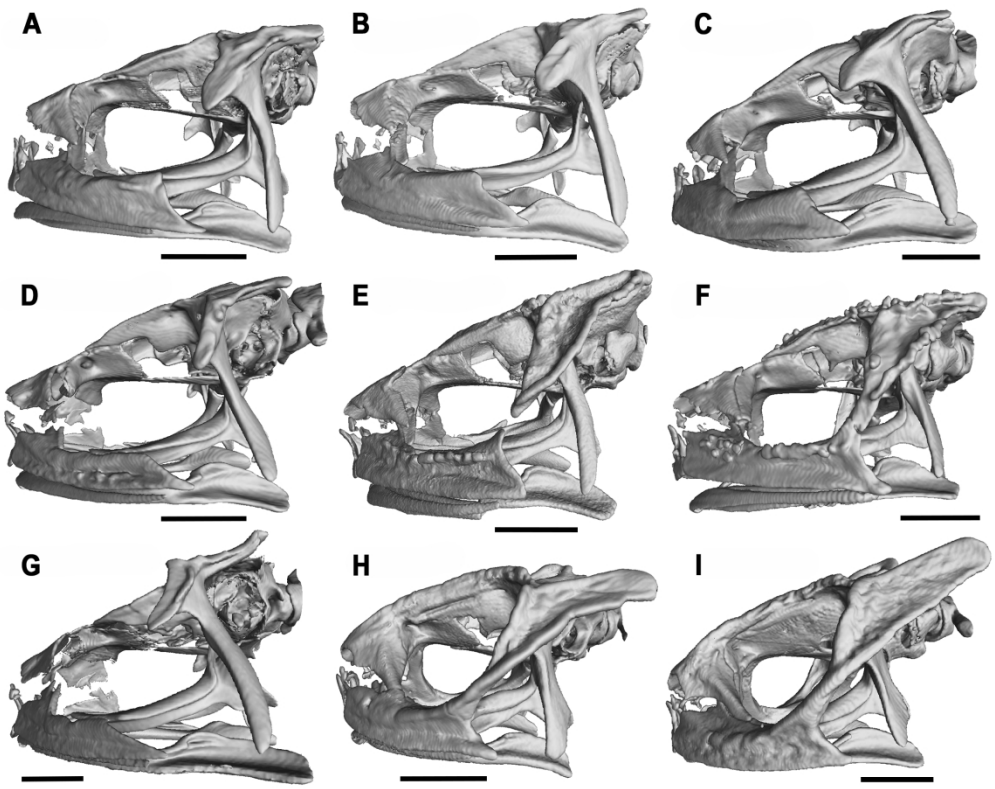

Figure 10

199x158mm (300 x 300 DPI)

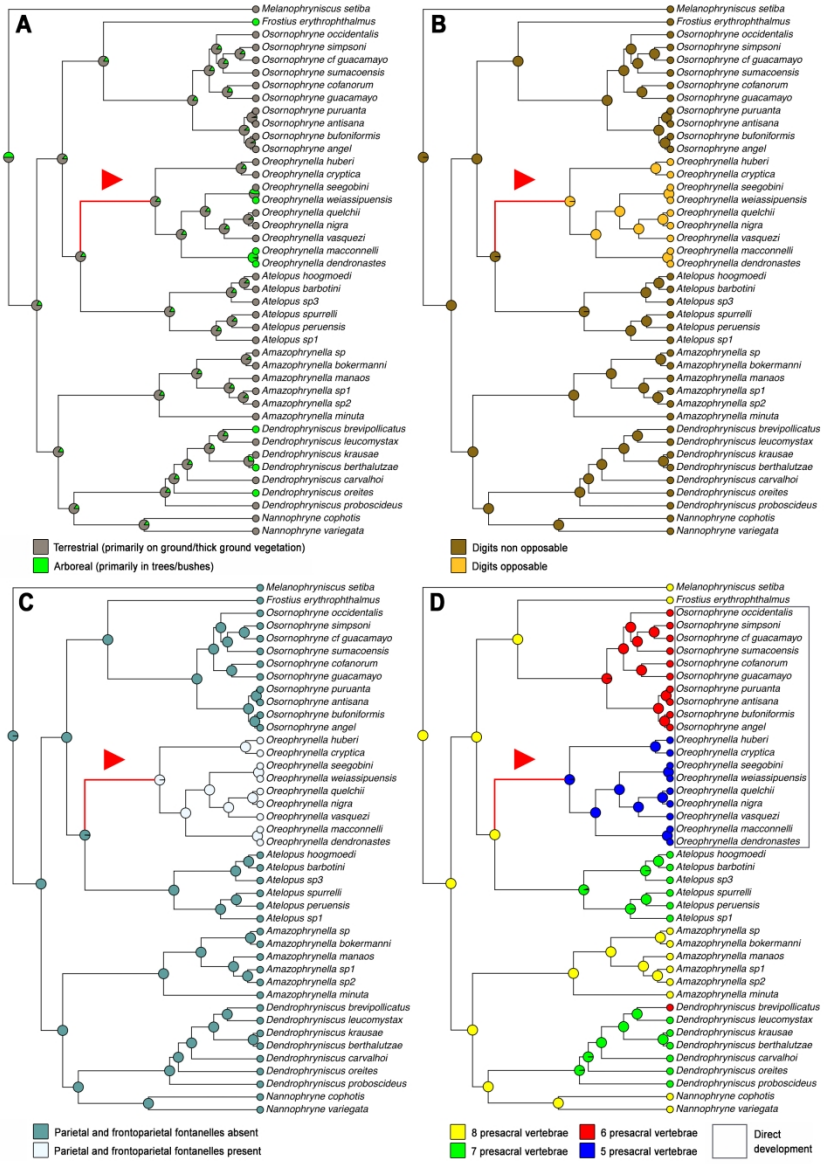

Figure 11

199x279mm (300 x 300 DPI)